UNIVERSIDADE D
COIMBRA

Cristiana Viseu Leote

Dissecting the Mechanisms Underlying the Anti-Inflammatory Effects of Sitagliptin on Microglial Cells

Dissertação no âmbito do Mestrado em Engenharia Biomédica, especialização em Neurociências, orientada pelo Doutor António Francisco Ambrósio e pela Doutora Hélène Léger, apresentada ao Departamento de Física da Faculdade de Ciências e Tecnologia, da Universidade de Coimbra.

setembro de 2023

UNIVERSIDADE D
COIMBRA

Cristiana Viseu Leote

Dissecting the Mechanisms Underlying the Anti-Inflammatory Effects of Sitagliptin on Microglial Cells

Dissertação no âmbito do Mestrado em Engenharia Biomédica, especialização em Neurociências orientada pelo Doutor António Francisco Ambrósio e pela Doutora Hélène Léger, apresentada ao Departamento de Física da Faculdade de Ciências e Tecnologia, da Universidade de Coimbra.

setembro de 2023

Execution of this work was supported by:

Foundation for Science and Technology (FCT), Portugal, Strategic Project (UIDB/04539/2020 and UIDP/04539/2020)

Agradecimentos

Antes de mais, começo por agradecer à Universidade de Coimbra pela oportunidade de frequentar o Mestrado em Engenharia Biomédica, pelos conhecimentos transmitidos e pelas experiências que me permitiu vivenciar, bem como ao *Retinal Dysfunction and Neuroinflammation Lab*, e ao Instituto de Investigação Clínica e Biomédica de Coimbra (iCBR), da Faculdade de Medicina da Universidade de Coimbra, por me terem permitido desenvolver a dissertação de mestrado e deixar a minha marca na sua história.

Aos meus orientadores, Doutor António Francisco Ambrósio e Doutora Hélène Léger, pela orientação científica, entusiasmo, confiança, ensino e paciência ao longo destes meses de trabalho. Um agradecimento especial à Doutora Hélène por ter sido imensamente paciente comigo, por me ter transmitido todos os conhecimentos técnicos e experimentais, e ensinamentos da melhor forma e por ter sempre acreditado em mim, nas minhas capacidades e no facto de que, mesmo com tantas adversidades, iríamos conseguir obter resultados. Não poderia ter tido uma orientadora melhor.

Obrigada à Lucia Bufano, estudante Erasmus, por todo o companheirismo, ajuda e trabalho em equipa que emergiram em resultados presentes nesta dissertação e numa amizade bonita, e à Beatriz Fazendeiro que desde o momento em que integrou no *Retinal Dysfunction and Neuroinflammation Lab* se tornou amiga, companheira de laboratório e uma grande ajuda ao longo do desenvolvimento deste trabalho.

Aos meus pais, um agradecimento especial e profundamente sentido por tudo o que me ensinam, por me darem a oportunidade de frequentar esta instituição secular e por me mostrarem, todos os dias, de que sou capaz de tudo se acreditar sempre em mim. Pais e irmã, sem vocês não teria sido possível. Muito obrigada por terem paciência para me suportar todos os dias, por me darem força nos dias mais difíceis, por acreditarem sempre, por nunca desistirem de mim e por serem três dos pilares mais importantes da minha vida.

Ao meu namorado, Leandro, um agradecimento do fundo do coração, por toda a ajuda, palavras de confiança e força, por acreditar e me fazer acreditar de que tudo é possível e por me apoiar em todos os momentos sem exceção. Obrigada por toda a paciência, dedicação e por seres um porto seguro ao longo deste tempo.

Obrigada aos quatro por nunca me deixarem ir abaixo e levarem este barco para a frente quando me faltavam forças.

Aos amigos que se tornaram família, Carla, João e Leandro, só tenho a agradecer por todas as palavras, apoio, confiança, fé e por estarem sempre lá quando eu mais precisei. Obrigada por existirem na minha vida e por me ajudarem tanto, mesmo quando não sabiam que o estavam a fazer.

Aos meus amigos de longa data, Rita e André, obrigada por permanecerem a meu lado, por terem sempre uma palavra de força e acreditarem tanto em mim.

À minha família, por todo o incentivo e apoio incondicional, por acreditarem que era possível, mesmo quando eu tinha dúvidas. Por todas as palavras de força, em todos os momentos e situações, o meu enorme obrigada.

A todas as pessoas que, direta ou indiretamente, contribuíram para o meu sucesso até à data, o meu sincero reconhecimento e agradecimento.

Por fim, mas não menos importante, agradecer às minhas duas estrelas (Avô Chico e Avó Fernanda), que me estão a ver onde quer que seja, por constantemente me protegerem e darem força para que consiga continuar a lutar contra todos os contratempos, pessoais e profissionais, nos dias bons e menos bons.

Obrigada a todos!

Contents

Figure List

Table List

Abbreviations

BCA	Bicinchoninic Acid Assay
BRB	Blood-Retinal Barrier
BSA	Bovine Serum Albumin
cDNA	Complementary Deoxyribonucleic Acid
CNS	Central Nervous System
COX-2	Cyclooxygenase 2
CT	Control
DEPC	Diethyl Pyrocarbonate
DNA	Deoxyribonucleic Acid
DPP4	Dipeptidyl Peptidase 4
DR	Diabetic Retinopathy
FBS	Fetal Bovine Serum
GCL	Ganglion Cell Layer
GIP	Glucose-Dependent Insulinotropic Polypeptide
GLP-1	Glucagon-Like Peptide-1
iBRB	Inner Blood-Retinal Barrier
ICAM-1	Intercellular Adhesion Molecule
IL-1β	Interleukin-1β
Il-6	Interleukin-6
Il-8	Interleukin-8
INL	Inner Nuclear Layer
iNOS	Inducible Nitric Oxide Synthase
IPL	Inner Plexiform Layer
KO	Knock-out
LB	Luria Broth
LPS	Lipopolysaccharide
oBRB	Outer Blood-Retinal Barrier
OCT	Optical Coherence Tomography
ONL	Outer Nuclear Layer
OPL	Outer Plexiform Layer
PBS	Phosphate-buffered Saline
PCR	Polymerase Chain Reaction

PNK	Polynucleotide Kinase
PVDF	Polyvinylidene Difluoride
RGCs	Retinal Ganglion Cells
RIPA	Radioimmunoprecipitation
RNA	Ribonucleic Acid
ROS	Reactive Oxygen Species
RPE	Retinal Pigment Epithelium
RPMI	Roswell Park Memorial Institute medium
RT	Room Temperature
RT-PCR	Reverse Transcription Polymerase Chain Reaction
RT-qPCR	Quantitative Reverse Transcription PCR
SEM	Standard Error of the Mean
sgRNA	Single Guide Ribonucleic Acid
Sita	Sitagliptin
TNF	Tumor Necrosis Factor
VEGF	Vascular Endothelial Growth Factor
WT	Wild Type

Resumo

A retinopatia diabética é uma doença neurovascular crónica associada à diabetes, sendo uma das principais causas de perda de visão e cegueira em adultos em idade ativa [1, 2]. As causas desta patologia residem predominantemente nos níveis elevados de glicose no sangue e na inflamação crónica da retina, tendo as células da microglia da retina um papel importante na inflamação [3–8]**.**

Em situações agudas, as células da microglia desempenham um papel duplo que inclui funções anti e pró-inflamatórias. Em condições de hiperglicemia crónica, ocorre inflamação persistente na retina, causando reatividade microglial permanente, perpetuando assim a lesão [2, 9–11]. Como resultado, citocinas pró-inflamatórias como o fator de necrose tumoral (TNF) e a interleucina-1β (IL-1β), quimiocinas e outros mediadores como a síntase induzível do monóxido de azoto (iNOS) contribuem para a patogénese da retinopatia diabética. Em indivíduos com diabetes, os níveis destas citocinas pró-inflamatórias e quimiocinas estão elevados, resultando em alterações e danos celulares na retina e na barreira hematorretiniana [12–17].

A dipeptidil peptidase 4 (DPP4) é uma exopeptidase de serina, com um papel importante na clivagem das hormonas incretinas, fatores de crescimento, citocinas e quimiocinas, participando assim em diversos processos fisiológicos, incluindo respostas imunes e regulação da inflamação [18–25].

A sitagliptina é um inibidor da DPP4 que inibe a clivagem de hormonas incretinas, conduzindo a um aumento dos níveis das mesmas, e consequentemente, da secreção de insulina e a uma diminuição da produção de glicose. Além disso, reportámos previamente que a sitagliptina tem efeitos protetores e anti-inflamatórios na retina diabética, inibindo o aumento dos níveis de citocinas pró-inflamatórias, o *stress* nitrosativo e a apoptose, bem como a rutura da barreira hematorretiniana. Além disso, a sitagliptina inibe o aumento da imunorreatividade da iNOS em células CD11b-positivas, em culturas primárias de células da retina e culturas organotípicas de retina, bem como as alterações morfológicas das células da microglia induzidas por exposição a lipopolissacarídeo (LPS) [26–28]. No entanto, os nossos resultados anteriores não demonstraram se a sitagliptina é capaz de inibir diretamente a reatividade da microglia.

Deste modo, este estudo foi realizado com o objetivo de 1) determinar se a sitagliptina pode exercer efeitos anti-inflamatórios diretamente nas células da microglia; e

2) verificar se esses efeitos dependem da inibição da DPP4 pela sitagliptina, ou se existem outros efeitos pleiotrópicos.

Para atingir os objetivos, utilizaram-se dois modelos *in vitro*: células BV-2, uma linha celular de microglia, e células BV-2 Dpp4 knock-out (KO). As experiências envolvendo a exposição de células BV-2 a LPS, na ausência ou presença de sitagliptina, produziram resultados significativos. A sitagliptina inibiu eficazmente o aumento dos níveis das proteínas iNOS, IL-1β e TNF, induzido pelo LPS, e inibiu o aumento da eficiência fagocítica detetada nestas células, quando expostas a LPS. Estes resultados fornecem evidências claras que suportam as propriedades anti-inflamatórias da sitagliptina e também o seu impacto direto nas células da microglia. A obtenção de células DPP4 KO foi bem sucedida, e verificou-se que a deleção de Dpp4 não alterou a morfologia das células. Os resultados com as células BV-2 Dpp4 KO revelaram que a sitagliptina não exerceu o seu efeito preventivo sobre o aumento da eficiência fagocítica induzido pelo LPS nestas células, indicando que o efeito da sitagliptina se deve, essencialmente, à inibição da DPP4.

Em conclusão, este estudo estabelece inequivocamente que a sitagliptina exerce uma influência direta nas células da microglia, e particularmente, efeitos anti-inflamatórios. No entanto, apesar dos resultados obtidos sugerirem que o efeito da sitagliptina é mediado pela inibição da DPP4, é necessário prosseguir com a investigação, de modo a determinar se as propriedades anti-inflamatórias da sitagliptina dependem exclusivamente da sua interação com a DPP4, ou se existem outros efeitos pleiotrópicos, que também poderão desempenhar um papel nos efeitos da sitagliptina.

Palavras-chave: Microglia, Inflamação; Sitagliptina; Dipeptidil peptidase 4; Retinopatia diabética.

Abstract

Diabetic retinopathy is a chronic neurovascular disease associated to diabetes, emerging as a primary driver of vision impairment and blindness among working-age adults [1, 2]. The origins of this condition lie predominantly in elevated blood glucose levels and enduring retinal inflammation, playing retinal microglial cells a significant role in inflammation [3–8].

In acute injury, microglia are prompted into action, engaging in a dual role of both anti-inflammatory and pro-inflammatory functions. Under chronic hyperglycemia, persistent inflammation occurs in the retina leading to a continuous microglial reactivity, perpetuating the injury [2, 9–11]. Consequently, pro-inflammatory cytokines, such as tumor necrosis factor (TNF) and interleukin-1β (IL-1β), chemokines, and other mediators like inducible nitric oxide synthase (iNOS) contribute to the pathogenesis of diabetic retinopathy. Among individuals with diabetes, these pro-inflammatory cytokines and chemokines are heightened, resulting in cellular failure in the retina and the disruption of the blood-retinal barrier (BRB). [12–17].

Dipeptidyl peptidase 4 (DPP4) is a serine exopeptidase, with an important role in the cleavage of incretin hormones, growth factors, cytokines, and chemokines, thus participating in diverse physiological processes, including immune responses and the regulation of inflammation [18–25].

Sitagliptin is a DPP4 inhibitor that inhibits the cleavage of incretin hormones, leading to an increase in their levels, and consequently insulin secretion and a decrease in glucose production. Beside this, we previously reported that sitagliptin has protective and anti-inflammatory effects in the diabetic retina, inhibiting the increase of pro-inflammatory cytokine levels, nitrosative stress, and apoptosis, as well as the breakdown of the BRB. Furthermore, it inhibits the lipopolysaccharide (LPS)-induced augmentation of iNOS immunoreactivity in CD11b-positive cells in retinal primary cell cultures and organotypic cell cultures, as well as microglial morphological changes triggered by LPS [26–28]. However, our previous data did not demonstrate whether sitagliptin is able to directly inhibit microglia reactivity.

Therefore, this study was undertaken with the aim of 1) determining whether sitagliptin can directly exert anti-inflammatory effects on microglial cells; and 2) establishing whether these effects were contingent upon the inhibition of DPP4 by sitagliptin, or if other pleiotropic effects might be at play.

To accomplish our aims, we used two *in vitro* models: BV-2 cells, a microglia cell line, and Dpp4 knock-out (KO) BV-2 cells. Our experimentation involving the exposure of BV-2 cells to LPS, in the absence or presence of sitagliptin, yielded significant findings. Sitagliptin effectively inhibited the LPS-induced upregulation of iNOS, IL-1β, and TNF protein levels, and it reduced the heightened phagocytic efficiency observed in these cells when exposed to LPS. These results provide strong evidence supporting the anti-inflammatory properties of sitagliptin and its direct impact on microglial cells. On the other hand, while we were successful in generating Dpp4 KO cells and ascertained that the deletion of Dpp4 did not alter the morphology of these cells, our investigations revealed that sitagliptin did not exert its preventive effect on the LPS-induced increase in phagocytic efficiency in the Dpp4 KO cells, indicating that the effect of sitagliptin was essentially due to DPP4 inhibition.

In conclusion, this study unequivocally establishes that sitagliptin exerts a direct influence on microglial cells, and particularly anti-inflammatory effects. Despite the results obtained suggesting that the effect of sitagliptin is mediated by the inhibition of DPP4, further investigation is needed to determine whether the sitagliptin anti-inflammatory properties are exclusively dependent on its interaction with DPP4, or if there are other pleiotropic effects, that might also play a role.

Keywords: Microglia; Inflammation; Sitagliptin; Dipeptidyl peptidase 4; Diabetic retinopathy.

CHAPTER 1

Introduction

1. Introduction

1.1. The eye

The eye is the organ responsible for capturing images from the environment and initiating the process of vision, which allows for the perception of information transmitted by the observed images. Both the structures and functions of the eye are quite complex, as each eye constantly needs to adjust the amount of light allowed in, focus on objects whether they are near or far, and produce electrical signals from the captured light to be transmitted to the brain, where they will be processed and transformed into continuous visual images [3, 29].

The eye is composed of three main layers of tissue - the external or fibrous, the intermediate, and the internal or nervous - with only the internal layer containing light-sensitive neurons capable of transmitting visual signals. This layer is also known as the retina [30].

The external layer is composed of the cornea and the sclera, whose main function is to protect the eye. The sclera is the outer, white, opaque, fibrous membrane composed of collagen fibers that cover and protect the eyeball. The cornea is the most important lens of the eye, being thin, resistant, transparent, and avascular, allowing the entry of light rays into the eyeball through the pupil [4, 31].

The intermediate layer includes the iris, ciliary body, and choroid. The iris, better known as the circular and coloured part of the eye, surrounds the pupil and its main function is to control the amount of light entering the eye, allowing a variable amount of light to enter through the dilation and contraction of the pupil to adapt to the brightness of the environment. The ciliary body is a muscular structure that surrounds the lens and changes its shape during the focusing process, allowing the eye to accommodate the image it is seeing. This structure also produces aqueous humor, a fluid that provides the necessary nutrients to the eye [6]. The choroid is the tissue layer located between the retina and the sclera, responsible for nourishing the retina's photoreceptors through the blood vessels present in it [4, 30].

The retina is the only nervous tissue of the eye that, through light-sensitive photoreceptors, converts light into electrical signals and then sends these nerve impulses to the brain through the optic nerve [30, 32].

1.2. The retina

The retina is divided into five neuronal classes, which are organized into three main cellular layers - the outer nuclear layer (ONL), the inner nuclear layer (INL), and the ganglion cell layer (GCL), separated by two synaptic layers - the outer plexiform layer (OPL) and inner plexiform layer (IPL) (Figure 1) [33, 34].

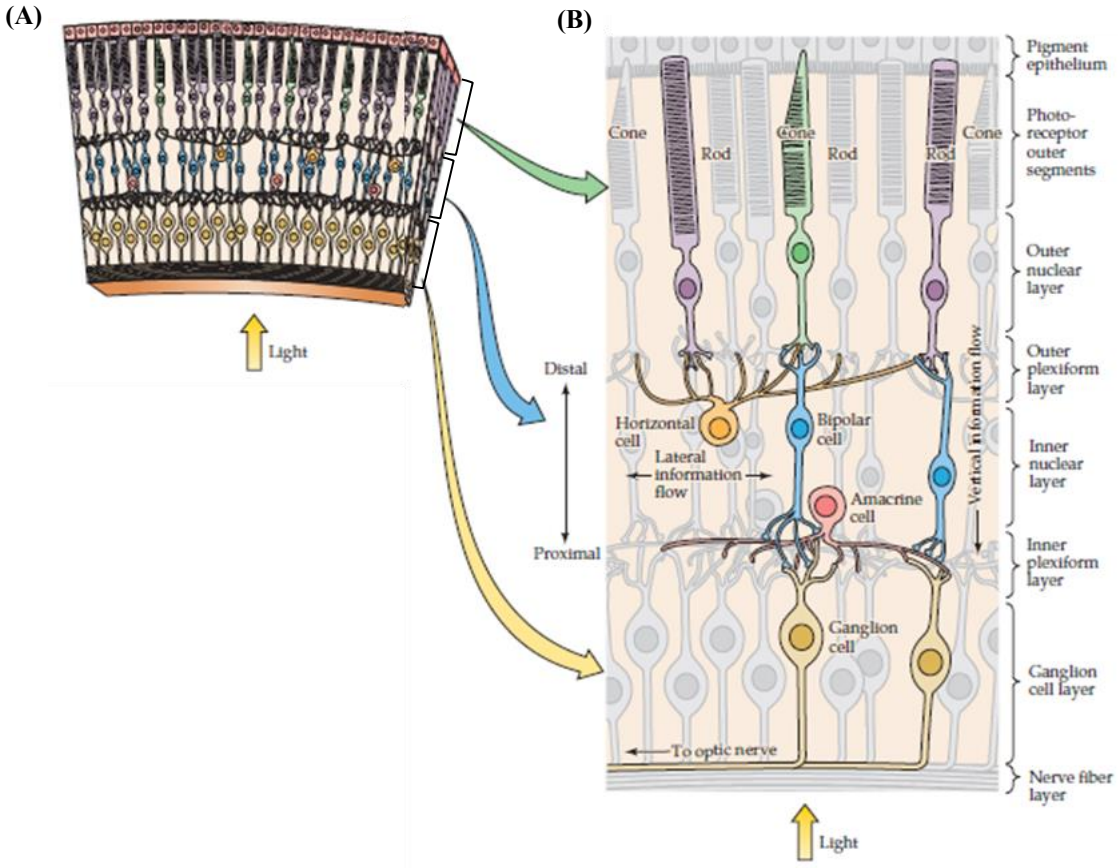

Figure 1 - Structure of the retina. (A) Section of the retina showing the overall arrangement of the retinal layers. (B) Diagram of the basic circuitry of the retina. Adapted from [38].

The ONL is composed of photoreceptors that can be divided into rods and cones, which are responsible for light detection. The photoreceptors have the main function of converting light signals into nerve impulses, which are subsequently transmitted by the bipolar cells, the ganglions cells, and the optic nerve to the lateral geniculate nucleus, in the humans, or to the superior colliculus in rats, and, subsequently, to the visual cortex, which is in the back of the brain. There are two types of photoreceptors, rods, and cones. Rods are the most numerous (estimated to be 120 million per eye in humans), mainly distributed in the periphery of the retina, allowing a minimum perception of objects under conditions of very low luminosity, but without allowing their distinction [35]. Cones (6 million per eye in

humans), located mainly in the central region of the retina (also known as the macula), have the function of allowing vision in conditions of high luminosity, as well as the visualization of colours and visual acuity. This type of cell is responsible for detailed object vision [35].

The photoreceptors establish synapses with the dendrites of the bipolar cells and horizontal cells. These cells, as well as the amacrine, and the Müller cells are the main constituents of the inner nuclear layer (INL) [33].

The retinal pigment epithelium (RPE) is a layer of single hexagonal, polarized, and pigment-containing cells that holds great significance in the retina due to its multifunctional and structural properties. It acts as an outer blood-retinal barrier and carries out essential metabolic activities that are crucial for maintaining and supporting the photoreceptors and overall visual function [36, 37]. RPE perform several critical functions, including eliminating metabolites (CO_2 and lactate) produced by active photoreceptors, phagocytosing the outer segments of photoreceptors, and also secreting angiogenic and angiostatic cytokines in order to maintain the confluency and permeability of the blood vessels of choroid [38].

The bipolar cells are postsynaptic to rods and cones, allowing communication between photoreceptors and ganglion cells [39].

The horizontal cells play a role in connecting bipolar cells to one another, thus regulating the flow of information between photoreceptors and bipolar cells in the outer plexiform layer (OPL) of the retina. Additionally, horizontal cells can form connections directly with photoreceptors and can synapse with both photoreceptors and bipolar cells. Furthermore, these cells are responsible for facilitating eye adjustment, ensuring consistent visual acuity regardless of changes in lighting conditions. [35, 40, 41].

The amacrine cells, like horizontal cells, integrate and modulate the flow of information presented to the ganglion cells by releasing neurotransmitters [35].

The outer plexiform layer (OPL) contains axons and nerve terminals of rods and cones, as well as dendrites of horizontal and bipolar cells, and is the site where synapses occur between these structures. Meanwhile, the inner plexiform layer (IPL) also contains axons and nerve terminals of bipolar cells and dendrites of ganglion and amacrine cells, allowing for synapse between them [35, 40, 41].

The ganglion cells layer (GCL) contains the retinal ganglion cells and amacrine cells. The ganglion cells are responsible for receiving visual signals from the bipolar and amacrine cells and transmitting them to the brain through their axons [32]. The axons of ganglion cells group in nerve fibers and form the optic nerve [39].

1.3. The blood-retinal barrier

The blood-retinal barrier (BRB) has two components, the inner BRB (iBRB) and the outer BRB (oBRB) (Figure 2) and plays a crucial role in the retina. The BRB controls the retinal microenvironment by regulating the fluids and molecular movements between the retinal vasculature, the choroidal vessels, and retinal tissue, effectively preventing the entry of macromolecules and potentially harmful substances in the retina. In this way, the BRB functions as a physiological barrier capable of controlling the flux of ion, protein, and water into or out of the retina [42–44].

The iBRB is constituted mainly by endothelial cells of retinal vessels that build tight junctions, forming a barrier along the vasculature of the inner retina. These vessels supply blood to the retina up to and including the OPL, while the photoreceptor cell layer remains devoid of blood vessels. The activity of the iBRB can be directly influenced by regulatory signals sent by astrocytes, Müller cells, and pericytes, but also by microglial cells and neurons, in response to changes in the microenvironment of the retinal neuronal circuit [42–45].

The oBRB is composed by the RPE cells, which are also connected by tight junctions. Its primary functions include the regulation of nutrients access from the blood to the photoreceptors, the elimination of waste molecules from the outer retina, and ensuring the retinal adhesion [42–45].

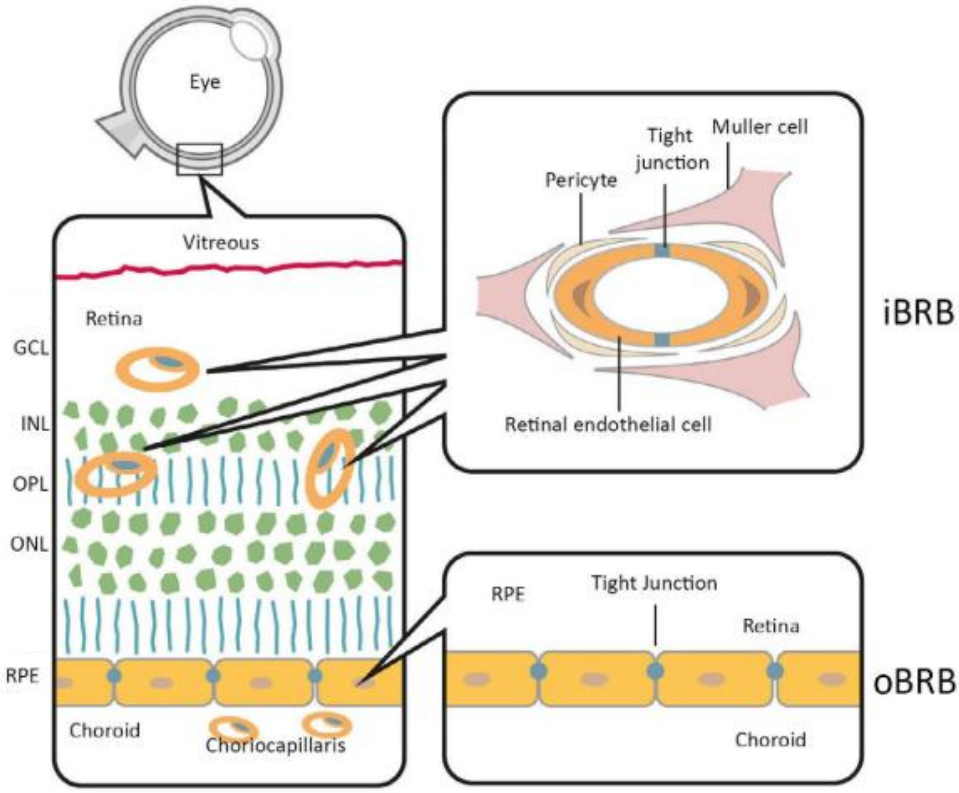

Figure 2 - Anatomic localisation of the blood-retina barriers. iBRB is formed by the blood vessels that supply the retina. oBRB is constituted by the RPE. Adapted from [46]. GCL: ganglion cell layer; INL: inner nuclear layer; OPL: outer plexiform layer; ONL: outer nuclear layer; RPE: retinal pigment epithelium.

1.4. The retinal glial cells

Retinal glial cells are usually divided into macroglia (Müller cells and astrocytes) and microglia. They can be activated when the retina is exposed to stress or damaged, initially releasing various biologically active molecules to promote tissue repair [46].

1.4.1. The Müller cells

The Müller cells are the most prevalent glial cells in the retina. They have their cell bodies located in the INL, and their axons extend throughout all layers of the retina, thus enabling the formation of supportive structures. These structures are crucial to the proper functioning of the retina, as they ensure the survival of photoreceptors and other retinal neurons, guide light to the photoreceptors, provide structural support, regulate immune and inflammatory responses, as well as supply neurons and photoreceptors with essential nutrients. Moreover, the Müller cells play a key role in maintaining the microenvironment

of the retina by controlling the ionic composition of the extracellular fluid and removing neurotransmitters from the synapse after their release, among other functions [47, 48].

1.4.2. The astrocytes

The astrocytes have multiple functions in the retina, including the regulation of local blood flow, the contribution for the normal function of neurons and retinal blood vessels. Importantly, astrocytes participate in the formation and maintenance of the BRB. They play a crucial role in the development and proper functioning of the retina by providing neurotrophic support for neurons, protecting them from toxins and injuries, and offering mechanical support to damaged neurons. Astrocytes also maintain the microenvironment by removing excess potassium and neurotransmitters from the synaptic cleft [48, 49].

1.4.3. The microglia

Microglial cells promote the surveillance of the central nervous system (CNS) environment, including the retina, and play a crucial role in the immune-mediated protective mechanisms. These cells can exhibit different phenotypes, such as a ramified morphology with a small cell body and long, thin processes under healthy conditions, to survey the environment, or a reactive state, under injury situations, where they appear more ameboid with enhanced phagocytic and migration capacity. In such circumstances, microglial cells are capable of migrating to the site of injury, proliferating and releasing cytokines, chemokines, nitric oxide (NO), reactive oxygen species (ROS), and other factors [9].

Due to the presence of sensitive molecules, such pattern recognition receptors, cytokine and chemokine receptors on their surface, microglial cells can identify pro-inflammatory mediators, leading to increased microglial activation. This contributes to ongoing inflammation processes that attempt to combat the injury process [9, 10, 32].

However, in neurodegenerative diseases, the activation of microglia may become chronic, and this excessive reactivity of microglia can be one of the main reasons for the progression of the those diseases [9].

Under normal healthy conditions in the retina, microglial cells are primarily found in the synapses-rich layers, IPL and OPL, while being absent in the photoreceptor cell bodies layer, the ONL, and sparsely populated in the INL [29].

In their non-reactive state, microglial cells play a crucial role in maintaining a healthy environment by phagocytosing cellular debris and releasing mediators that support the survival of retinal cells [29].

Upon activation in response to injury, these cells exhibit a higher capacity to phagocytose apoptotic cells and cellular waste. They also release pro-inflammatory mediators, such as nitric oxide, and cytokines, like tumor necrosis factor (TNF), interleukin (IL)-1β and IL-6, chemokines, and reactive oxygen species (ROS). Elevated levels of these pro-inflammatory factors can lead to an overactive immune response, resulting in neuronal and retinal damage [2, 9–11, 32, 50].

1.5. Diabetic retinopathy

Diabetic retinopathy (DR) is the leading cause of vision loss and blindness in working-age adults, in individuals with diabetes, including those with type 1 or type 2.

World Health Organization estimates that more than 422 million people worldwide had diabetes, representing 8.5% of the adult population and the prevalence tends to rise every year. According to the National Eye Institute, over half of diabetic individuals will develop diabetic retinopathy, but controlling blood glucose levels can reduce the risk of developing this condition. The risk of developing diabetic retinopathy increases with the duration of diabetes [3, 4, 30].

Diabetic retinopathy had been considered for many decades a microvascular disease of the retina, but nowadays, based on increasing evidence obtained from many human and animal studies, it is considered a chronic neurovascular disease.

1.5.1. The vascular dysfunctions observed in diabetic retinopathy

Hyperglycemia and altered metabolic pathways in diabetes leads to retinal microglial and endothelial cell dysfunction (Figure 3) [1, 2]. Regarding the microvascular disease, diabetic retinopathy has two main stages: nonproliferative retinopathy and proliferative retinopathy [2, 8]. In nonproliferative retinopathy, which is the early stage of the disease, blood vessels can leak or bleed [8]. This stage is characterized by three subtypes: mild (presence of small areas of inflammation), moderate (blood vessels obstruction and increased vascular permeability, due to inflammation), and severe (blood vessels blocking).

The advanced stage of the disease is called proliferative retinopathy. It is characterized by the atypical growth of novel weak blood vessels on the retina's surface that leak or bleed easily, which may lead to vitreous hemorrhages causing severe vision loss or blindness [4, 8, 31, 51].

The early detection of the disease increases the chances of successful treatment. However, it is impossible or very difficult to detect the early and mild stages of the nonproliferative retinopathy. Thus, to prevent the advance of the disease before the appearance of retinal dysfunction and damage. Although there is currently no cure for diabetic retinopathy, there are several treatment options available, which are targeted for the later stages of the disease, that can delay or reduce vision loss. These include photocoagulation, or laser treatment, which, although it is not much used nowadays in developed countries, it is believed to have a direct effect on closing leaking microaneurysms, improving oxygenation, and stimulating retinal pigment epithelium. Another option is vitrectomy, which involves surgically removing the injured vitreous gel and replacing it with a silicone oil bubble. Additionally, anti-vascular endothelial growth factor (VEGF) injections can be administered to slow down, stop, or prevent the growth of irregular retinal blood vessels, as vascular endothelial growth factor is known to trigger their growth [3–8].

However, these strategies have limitations and may not provide definitive solutions. With laser treatment, patients experience peripheral visual field loss and delayed dark adaptation. While anti-VEGF injections can help prevent the progression of diabetic retinopathy, they require frequent administration and monitoring. Unfortunately, the cost of regular clinic visits and anti-VEGF medications is very high. Vitrectomy is considered the last option for this condition, as it carries the potential risk of permanent vision loss due to complications such as retinal detachment or ischemic alterations [12].

1.5.2. Neuronal dysfunction and neurodegeneration

The dysfunction of vascular, neuronal, and glial elements in diabetic retinopathy has been the subject of numerous scientific investigations, and there is evidence suggesting their interdependence and importance for the pathology's development and progression (Figure 3). Neuronal dysfunction and neurodegeneration has emerged as an early event in the pathogenesis of DR, possibly interconnected with the microvascular anomalies observed during the pathology's progression [52, 53].

Glutamate excitotoxicity, loss of neuroprotective molecules, reactive gliosis, apoptosis of neural cells, diminished retinal neural function, are five features of diabetes-induced neuroglial dysfunction/degeneration observed in experimental models of DR. These aspects often precede the frequently described microangiopathy characteristic of this condition [52, 53].

So far, optical coherence tomography (OCT) has been employed to demonstrate the thinning of inner retinal layers, such as the retinal nerve fiber layer, ganglion cell layer, and to varying extents, the inner plexiform layer, in patients with either type 1 or type 2 diabetes without diagnosed DR. This thinning holds particular relevance as retinal ganglion cells and amacrine cells, along with photoreceptors, represent the first neurons to exhibit diabetes-induced apoptosis. Consequently, early neuronal dysfunction in DR contributes to its development and progression. The alterations in inner retinal thickness and the visual function impairments hint at the potential interdependence or cooccurrence of the neurodegenerative component of the pathology alongside vascular manifestations [52–54].

1.5.3. Inflammation in diabetic retinopathy

In addition to hyperglycemia, inflammation is a critical factor in the development of diabetic retinopathy (Figure 3). Inflammation is a non-specific reaction to injury, involving molecular mediators, such as anti and pro-inflammatory factors [12, 13]. Chronic inflammation is a known consequence and associated risk of prolongated hyperglycemia triggered by cell death and increased oxidative stress. Diabetic retinopathy is characterized by a low-grade chronic inflammation due to the chronic microglia reactivity, leading to the secretion of pro-inflammatory cytokines, e.g., TNF, IL-1β, IL-6, and chemokines, e.g., IL-8, and upregulation of inducible nitric oxide synthase (iNOS) and cyclooxygenase-2 (COX-2), and other factors such as NF- κB [13–15]. In diabetic patients, increased levels of TNF have been found in the vitreous fluid and retina, which is correlate with the severity of their pathology [12, 32]. Animal studies have also demonstrated that TNF induces endothelial dysfunction by producing ROS, leading to leukocyte adhesion and breakdown of the blood-retinal barrier [32]. Other pro-inflammatory factors, including IL-1β and iNOS, are also upregulated in the diabetic retina [15, 16]. iNOS has been shown to play a crucial role in blood-retinal barrier breakdown and diabetic retinal cell death, contributing to the development of diabetic retinopathy, as it is associated with the initiation of early vascular alterations in diabetes [16, 17, 32]. Furthermore, evidence has shown that IL-1β not only contributes to the breakdown of the BRB through its association with the accelerated

apoptosis of diabetic retinal endothelial cells but also by activating various types of cells that initiate an inflammatory signalling cascade, being this way associated to an important role in the involvement of innate immunity and contributing directly for this disease [2, 13].

1.5.4. Microglial changes in diabetic retinopathy

Microglial reactivity in the early stages of diabetic retinopathy have been linked to the low-grade pro-inflammatory state in the retina, but alterations in microglial behaviour during advanced pathology are also relevant [55, 56]. Microglial reactivity entails a change in their phenotype, in which these cells display both pro and anti-inflammatory actions. Early in the disease, the anti-inflammatory responses coincide with the pro-inflammatory actions, trying to mitigate inflammation and slowing the disease progression. However, as the disease advances, the anti-inflammatory actions diminish, allowing pro-inflammatory actions to persist and chronically activate pro-inflammatory signalling pathways. Thus, diabetes-related retinal inflammation has an increasingly recognized pathological role, supported by growing evidence from studies demonstrating that microglial activation in cell cultures and diabetic animal models leads to increased expression of pro-inflammatory factors (cytokines and chemokines) and subsequent induction of neuronal dysfunction and cell death [52–54, 57].

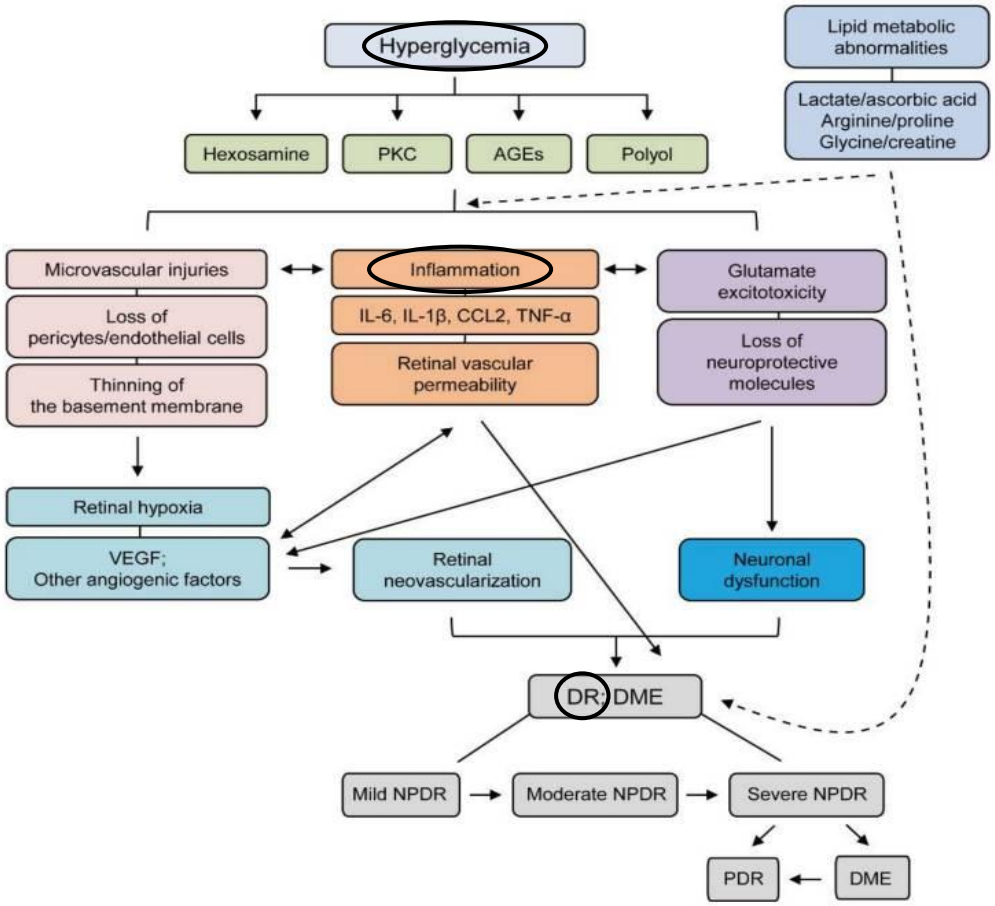

Figure 3 - Pathophysiology of Diabetic Retinopathy. Adapted from [12]. PKC: protein kinase C; AGEs: advanced glycation end products; DR: diabetic retinopathy; DME: diabetic macular edema; NPDR: non-proliferative diabetic retinopathy; PDR: proliferative diabetic retinopathy.

1.6. Sitagliptin, an inhibitor of dipeptidyl peptidase 4

Sitagliptin was approved and introduced to the market in the USA, as Januvia, in 2006. It holds the distinction of being the first dipeptidyl peptidase 4 (DPP4) inhibitor authorized for use as an oral antihyperglycemic medication for treating type 2 diabetes [58]. In more than 130 countries, sitagliptin is already approved as a therapy, alone or combined with other drugs, and it is taken, usually, once a day, having a low risk of pharmacokinetic drug interactions, being safe and with high levels of efficiency. Sitagliptin prevents the cleavage and subsequent degradation of incretin hormones [e.g., glucagon-like peptide-1 (GLP-1) and glucose-dependent insulinotropic polypeptide (GIP)], therefore increasing their levels, which leads to a stimulation of insulin secretion and a decrease of the glucose production. In other words, sitagliptin allows a better blood glucose control (Figure 4) [39, 59–61].

Sitagliptin belongs to the gliptins class, a set of anti-hyperglycemic agents that have been synthesised and used in clinics. It contains a β-amino acid scaffold, which allows sitagliptin to selectively connect and inhibit DPP4 (Figure 5) [26, 62].

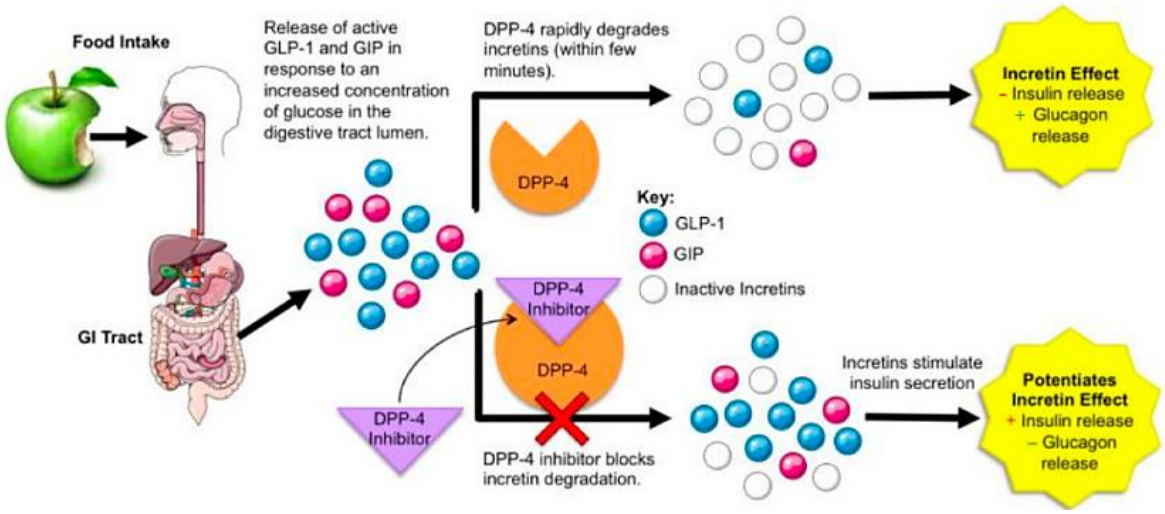

Figure 4 - DPP4 function and DPP4 inhibitors' mechanisms of action. Adapted from [28]

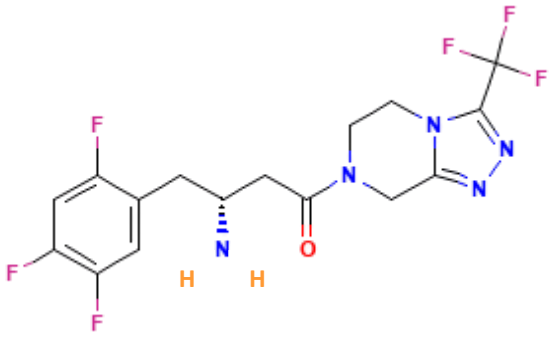

Figure 5 - Sitagliptin structure. Adapted from [62].

1.6.1. Dipeptidyl peptidase 4

DPP4, also known as CD26, is a 110 kDa protein that can be present in two different forms, a type II transmembrane glycoprotein and a cleaved and soluble form, present in blood plasma and others body fluids (Figure 6) [18]. This protein can be localized in many tissues and cell types, such as neural, in specific glial cells (microglia and astrocytes), endocrinal, gastrointestinal, pancreatic, respiratory tissues, and immune cells [63]. DPP4 is a serine exopeptidase, first studied for its ability to cleave the incretin hormones GLP-1 and GIP, thus regulating their levels. Moreover, DPP4 plays a role by cleaving many other dipeptides such as chemokines, cytokines, or neuropeptides. Finally, DPP4 attaches to many binding proteins, such as adenosine deaminase (ADA), CD45, fibronectin, caveolin-1, among others. Therefore, DPP4 is involved in many physiological processes [63]. DPP4 can regulate the activation of several immune cell types such as T-cells, their migration, and cytokine production. Moreover, DPP4 can cleave growth factors, potentially impacting their bioactivity and signalling pathways, which also by interacting with immunomodulatory peptides involved in immune responses, have an influence on the inflammatory response regulation [19–25, 63]. Overall, DPP4 is considered a regulator of immune responses and inflammation.

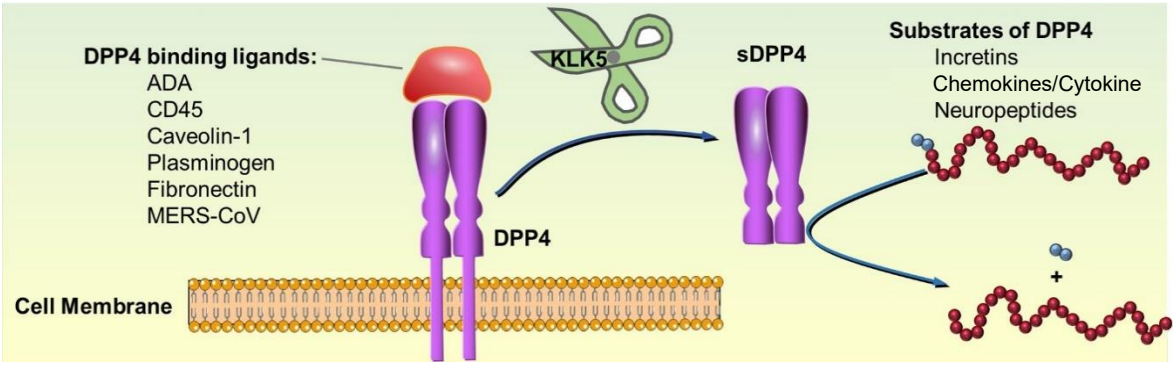

Figure 6 - DPP4 isoforms. Adapted from [18]. sDPP4: soluble DPP4.

1.6.2. Beneficial effects of sitagliptin

During the last decade, our group was the first demonstrating that sitagliptin has protective effects in the retina. In a rat model of type 2 diabetes (Zucker Diabetic Fatty rats), we demonstrated that sitagliptin prevents the redistribution and intracellular accumulation of tight junction proteins, such as occludin and claudin-5, thereby inhibiting changes in tight junctions. Furthermore, sitagliptin prevents the increase in inflammation, and particularly the levels of pro-inflammatory cytokines and intercellular adhesion molecule (ICAM-1), in the retina, as well as nitrosative stress and apoptosis [26]. We also demonstrated that sitagliptin can prevent BRB breakdown in a rat model of type 1 diabetes independently of the glycemia regulation. [26, 27, 46]. Furthermore, our group has also verified, in primary retinal cell cultures and organotypic retinal cell cultures, that sitagliptin not only significantly reduces the increase in iNOS immunoreactivity and nitrite levels in CD11b-positive cells (likely microglial cells) exposed to LPS, but also prevents the alterations in CD11b-positive cells morphology triggered by LPS, suggesting that sitagliptin presents potential anti-inflammatory effects [28]. However, we had no evidence that the anti-inflammatory effects observed in microglial cells were due to a direct effect of sitagliptin on these cells.

Main goals

Diabetic retinopathy is a non-curable neurovascular disease that commonly affects individuals with diabetes. A large body of evidence, including by our group, has shown that a chronic low-grade neuroinflammation mediated, at least in part, by microglial cells, plays a crucial role in the development and progression of diabetic retinopathy and other retinal degenerative diseases [15, 64–67].

Although there are some treatments available for this disease, they are not very effective in many patients. They are mainly targeted for the later stages of diabetic retinopathy and have several adverse effects. Therefore, there is an urgent need to develop novel treatments, particularly for the early stages of the disease that could at least to halt or delay its progression.

Sitagliptin is currently used as an oral antidiabetic medication to control blood glucose levels in patients with type 2 diabetes. Sitagliptin exerts its effect by inhibiting the DPP4 enzyme, thereby increasing the levels of incretins and, consequently, insulin levels.

Extensive research has been conducted on sitagliptin effects using cellular and animal models, both in type 1 and type 2 diabetes. Our group was the first demonstrating significant protective effects of sitagliptin in the retina, both in type 1 and type 2 diabetic animal models. In type 1 diabetic animals, the protective effects were independent of the glycemic control. In this case, the animals were not able to produce insulin and the glycemic levels were very high. Moreover, sitagliptin presented protective effects against the blood-retina barrier breakdown, and anti-inflammatory effects in the retina, namely by reducing the levels of IL-1β and ICAM-1 [26, 46]. Unpublished data from our group shows that sitagliptin is able to inhibit microglia reactivity in retinal primary mixed cultures and organotypic cultures. However, we do not have clear evidence that these anti-inflammatory effects on microglial cells were due to direct effects on these cells.

Therefore, considering the previous findings from our group, the main goals of this thesis are to 1) elucidate whether sitagliptin can exert direct anti-inflammatory effects on microglial cells; and 2) clarify whether those effects are dependent on the inhibition of DPP4 by sitagliptin, or if other pleiotropic effects can be involved.

CHAPTER 2

Materials & Methods

2. Materials & Methods

2.1. BV-2 cell line

BV-2 cells, derived from raf/myc-immortalized C57/BL6 mouse neonatal microglia, have been extensively employed in scientific research as a prominent microglial cell line. They resemble primary microglial cells in terms of both morphology and functionality, displaying similar reactivity and exhibiting an inflammatory response when exposed to LPS [68–70].

In situations where human cell availability is limited and considering the adherence to the principles of reduction, replacement, and refinement (3 R's), using commercially available immortalized mouse microglial lines becomes an option for advancing neurological research. BV-2 cells, therefore, serve as a valuable experimental model for researching the mechanisms underlying neuroinflammation and degenerative diseases. Their application in studying anti-inflammatory drugs make them particularly relevant in this study [68–71].

2.2. Culture and exposure of BV-2 cells to sitagliptin and LPS

BV-2 cells were cultured in Roswell Park Memorial Institute (RPMI) medium 1640, supplemented with 10% fetal bovine serum (FBS), 1% penicillin-streptomycin antibiotics, and 1% L-glutamine, under 5% CO_2 and 95% humidity, at 37ºC. BV-2 cells were passaged at ≈ 1:30 dilution, every three days. The stock of BV-2 cells was from passage 4 and the cells were kept in culture until passage 25 at maximum, before being replaced by new stocks.

For experimental purposes, the cells were seeded in RPMI containing 2% FBS at a cell density of 1 x 10^4 cells/cm^2. After 18 h of cell seeding, the cells were incubated with 200 µM sitagliptin (Sigma-Aldrich, USA), 0.1 µg/ml LPS (Sigma-Aldrich, USA), and sitagliptin plus LPS, for 24 h. Sitagliptin was added 30 min before the incubation with LPS (Figure 7). Fresh medium was added to the cells before the treatment.

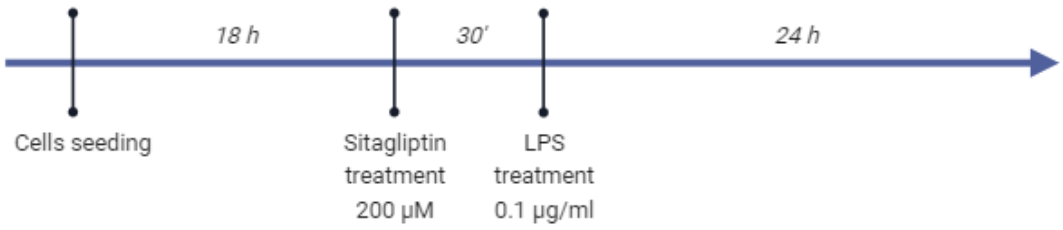

Figure 7 – BV-2 cells drug exposure protocol. Made with BioRender.

2.3. EdU assay

Cells were seeded in a 12-well plate containing coverslips (16 mm diameter). The cells were then treated with sitagliptin and LPS and incubated for 22 h. After that, 500 µl of the cell medium was removed from each well, and 500 µl of fresh medium containing 100 µM EdU (Click-iT™ EdU Cell Proliferation Kit for Imaging, Alexa Fluor™ 488 dye, ThermoFisher, Scientific, USA) was added. After a 2 h incubation, the medium was aspirated, and the cells were washed with 1x PBS and fixed with methanol at -20ºC for 10 min. Following another wash, the cells were permeabilized using 0.5% Triton X-100 for 20 min at room temperature (RT). Subsequently, the cells were washed with phosphate-buffered saline (PBS) + 3% bovine serum albumin (BSA). To detect cell proliferation, an EdU assay using Click-it chemistry with various fluorescent dyes was performed. The Click-it reaction cocktail was prepared by combining 430 µl of EdU reaction buffer (component D), 20 µl of CuSO4 (component E), 1.2 µl of Alexa Fluor 488 picolyl azide (component B), and 50 µl of EdU reaction additive at 1x concentration. The cells were then incubated with this cocktail for 30 min in a humidified chamber at RT, in the dark. After another wash with PBS + 3% BSA, the cells were stained with DAPI (1:10 000) at RT for 1 h. Finally, the cells were washed 3 times with PBS and mounted on slides using 10 µl of fluorescence mounting medium (DAKO, Denmark). Fluorescence microscopy (ZEISS, Germany) was used to capture images in five random fields per condition, and the images were subsequently analysed using ImageJ.

2.4. Apoptosis assay

Cell apoptosis was evaluated by immunocytochemistry, by assessing active (cleaved) caspase 3. Cells were seeded in a 12-well plate containing coverslips (16 mm diameter), and then incubated with sitagliptin, LPS and puromycin (1µg/ml; positive control). After 22 h, the cells were fixed with methanol at -20ºC for 10 min, permeabilized with PBS + 1% Triton X-100 for 5 min, and then blocked with PBS + 3% BSA + 0.2% Tween 20 for 1 h at RT. Primary antibody (anti-cleaved caspase 3; diluted 1:200 in PBS; Cell Signaling 9661 rabbit polyclonal, Cell Signaling, USA) was then added to the coverslips and incubated in a humidified chamber at RT for 1 h 30 min. After being washed three times, the coverslips were incubated with the secondary antibody (goat anti-rabbit; diluted 1:200 in blocking buffer; Alexa Fluor® 488 conjugate; Invitrogen, USA) for an additional hour, at RT. Finally, DAPI (1:2000; Invitrogen, USA) + phalloidin (1:500; Sigma-Aldrich, USA)

were incubated for 30 min, after which the coverslips were mounted on slides using fluorescence mounting medium (DAKO, Denmark). Fluorescence microscopy (ZEISS, Germany) was used to capture images in five random fields per condition, and the images were subsequently analysed using ImageJ.

2.5. Protein extraction and quantification

The bicinchoninic acid assay (BCA) method was employed to perform protein extraction. Cells were seeded in a 6-well plate and treated with sitagliptin and LPS. After 24 h, the cells were washed with PBS and scraped with radioimmunoprecipitation (RIPA) lysis buffer (100 µl/well; 150 mM NaCl, 50 mM Tris HCl, 5 mM EGTA, 0.5% sodium deoxycholate, 0.1% SDS, 1% Triton X-100, 0.1 mM DTT, milli-Q water until 100 ml; pH 7.5), supplemented with protease inhibitors (Roche, Germany). The resulting protein extracts were subjected to sonication (three times with 5 s pulses), incubation on ice for 30 min, and centrifugation (16 000x g for 10 min at 4ºC) in chilled Eppendorf tubes. A volume of 6 µl of each protein extract was transferred to a new tube, and Sample Buffer 6x (1:5, v: v) was added to the remaining volume of protein extract. The samples were denaturated at 95ºC and stored at -80ºC. Protein quantification was measured using the Pierce BCA Protein Assay Kit (ThermoFisher, Scientific, USA) with the 6 µl protein samples.

2.6. Western blot

The prepared leader and protein samples (20 µg per well) were added to each well of the acrylamide gel, stacked at 70V and raced at 140V for approximately 15 min and 1 h 30 min, respectively. During that time, the membranes were activated in methanol (2 min), water (2 min) and Transfer Buffer (5 min minimum). Once separated by size, the proteins were transferred to polyvinylidene difluoride (PVDF) membranes at 0.75 A, for about 1h 30 min, at 4ºC. Later, the membranes were blocked with 5% low fat milk / 0.1% Tris-buffered saline (TBS; 200 mM Tris HCl; 1.37 mM NaCl) supplemented with 0.1 % Tween 20 (TBS-T) for 1h. The membranes were incubated with the primary antibody overnight, at 4ºC on a shaker. After 3 washes with TBS-T, the membranes were then incubated with the secondary antibody for 1h and washed again 3 times with TBS-T for 10 min each. The membrane revelation and the image acquisition were performed with chemiluminescence detection machine (ImageQuant™ LAS 500, General Eletric, USA) [72].

2.7. Phagocytic assay

Cells were seeded in a 12-well plate containing coverslips (16 mm diameter) in RPMI + 2% FBS. After 18 h, the cells were treated with sitagliptin and LPS. Following 23 h of treatment, cells were incubated with 0.0025% fluorescent latex beads for 1 h (Sigma-Aldrich, USA). The cells were washed with PBS and fixed with methanol at -20ºC. After 10 min, the cells were permeabilized and blocked with 3% bovine serum albumin (BSA) + 1% Triton X-100 in PBS, for 30 min, stained with phalloidin-TRICT, diluted to 1:500 in PBS, for an additional 30 min. After staining, the cells were washed three times with PBS and stained with DAPI (diluted to 1:10 000 in PBS). After 30 min, the cells were washed with PBS and milli-Q water, and the coverslips were mounted with 10 µl fluorescence mounting medium (DAKO, Denmark) on glass slides. Fluorescence microscope images of 10 random fields were captured from each condition, and the phagocytic efficiency (%) was determined using the following formula [15]:

$$\text{Phagocytic efficiency (\%)} = \frac{\sum(1 \text{ x } x1 + \ 2 \text{ x } x2 + \ 3 \text{ x } x3 \ldots + \ n \text{ x } xn)}{\text{Total number of cells}} \times 100\%$$

xn represents the number of cells containing n beads (n = 1,2,3, ... up to a maximum of 6 points for more than 5 beads per cell).

2.8. Polymerase chain reaction (PCR) and reverse transcription PCR (RT-PCR)

The PCRs were performed on deoxyribonucleic acid (DNA) isolated from BV-2 cells while RT-PCRs were performed on complementary DNA (cDNA) from BV-2 cells. The PCR amplification was conducted according to the Supreme NZYTaq II 2x Green Master Mix protocol (NZYtech, Portugal) [73]. Each DNA or cDNA sample was mixed with Supreme NZYTaq II 2x Green Master Mix, primers (Table 1), and nuclease-free water. The amplification was carried out for 31 cycles using 200 ng of genetic material and 10 µM of forward and reverse primers. The amplification protocol consisted of an initial denaturation at 95ºC (5 min), followed by 31 cycles of denaturation at 94ºC (30 sec), annealing at the appropriate temperature (generally at 60ºC for 30 sec), and extension at 72ºC (20 sec), ending with a final extension at 72ºC for 5 min. The resulting samples were suitable for electrophoresis on a 1% agarose gel with 1% (v/v) green safe.

Table 1 - List of primers used for RT-PCR and RTq-PCR.

Gene	Primer Sequence
Dpp4	F3 ex11: 5'-CGTGAATCTGCCAAACTCCATG-3'
	R3 ex13: 3'-CGACGCGGGGTGCACT-5'
	F4: CTGAGCTACTCTACCTTACTG
	R2: GATCTGGCCATTTTCTCTCTTTAG
Gapdh	F31: CGACTTCAACAGCAACTC
	R33: TGTAGCCGTATTCATTGTCATA
Ywhaz	F34: CAGCAAGCATACCAAGAAG
	R35: TCGTAATAGAACACAGAGAAGT

2.9. CRISPR/Cas9 cloning

Benchling.com was utilized to design the single guide ribonucleic acid (sgRNA). To initiate primer annealing, the forward and reverse primers were combined at equal concentrations with T4 buffer, diethyl pyrocarbonate (DEPC) water, and T4 polynucleotide kinase (PNK) (New England BioLabs, USA). The mixture was incubated at 37ºC for 30 min, followed by a 5 min incubation at 95ºC. The temperature was then gradually reduced at a rate of 5ºC per min until reaching 25ºC, allowing for primer annealing and the formation of ds-gRNA. The resulting product was purified using the PureLinkTM Quick Gel Extraction and PCR Purification Combo Kit (Invitrogen, USA), following the manufacturer's protocol. Subsequently, 2 µg of pX459 plasmid was digested with the 1 µl BbS1 restriction enzyme (R0539S, New England BioLabs, USA) (Figure 8A). Complete digestion was ensured by running 100 µg on agarose 0.8% gel. The purified ds-gRNA was then ligated to the digested plasmid using T7 DNA ligase and the appropriate ligation buffer (M0318, New England BioLabs, USA) (Figure 8B). The ligation reaction was performed overnight at 16ºC. The pX459 plasmid contains resistance genes for both ampicillin and puromycin.

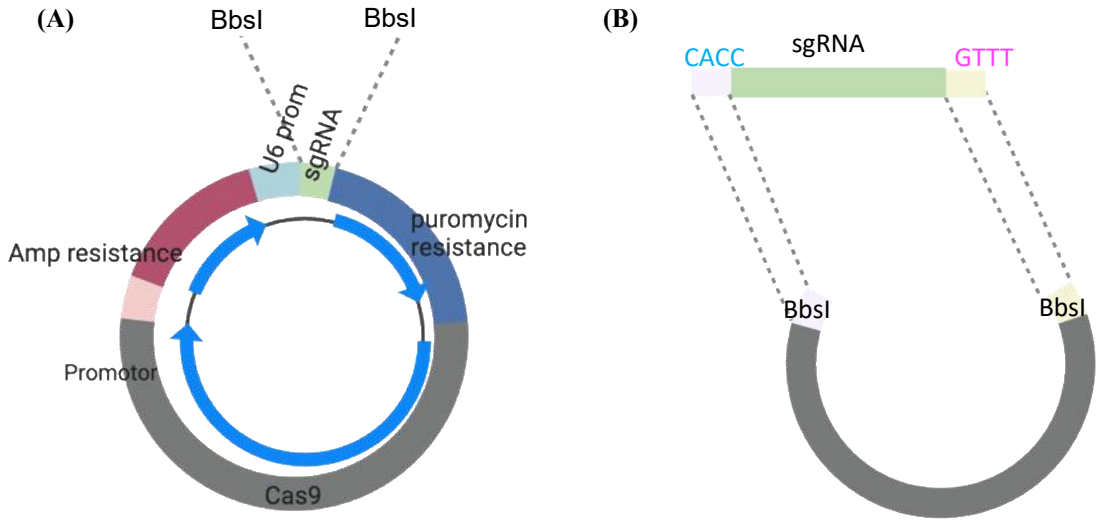

Figure 8 - CRISPR/Cas9 cloning. (A) pX459 plasmid digestion with BbsI restriction enzyme. (B) ds-sgRNA ligation to the plasmid by DNA ligase and ligation buffer. Made with BioRender.

Competent *E. coli* bacteria (dH5α, 18265017, Alfagene, Portugal) were transformed with the pX459 plasmid resulting from the ligation reaction and cultured on an agar + Luria broth (LB) plate. The transformed bacteria were selected by using ampicillin. Subsequently, the recombinant plasmid was isolated from the selected bacteria. The ds-gRNA and plasmid constructs were validated through bacterial sanger sequencing, from the U6 promoter using the U6-Fwd primer (Table 2).

Table 2 - Sequence of the oligos used to perform CRISPR/Cas9 cloning and transfection, and the primers.

Name	Sequence
sgRNA sequence	CAGCTAGTGAATACGTTCTG **CGG**
Top oligo	CACCGCAGCTAGTGAATACGTTCTG
Bottom oligo	AAACCAGAACGTATTCACTAGCTGC
U6-Fwd	GAGGGCCTATTTCCCATGATTCC
Dpp4 ex11 F3	CGTGAATCTGCCAAACTCCATG
Dpp4 ex12 R3	CGACGCGGGGTGCACT

2.10. Deletion of Dpp4

To perform transfection, cells were seeded in a 6-well plate, at a concentration of 8 x 10^4 cells/well. The Lipofectamine™ 3000 Transfection Reagent (L3000015, Alfagene, Portugal) protocol was followed, which requires 2500 ng of DNA, 5 µl of P300 and 7.5 µl of lipofectamine 3000 reagent for a 6-well plate [74]. Mix 1, consisting of 125 µl of OptiMEM and 7.5 µl of lipofectamine 3000 reagent, was combined with mix 2, which contains 125 µl of OptiMEM, 2.5 µg of plasmid pX459, and 5 µl of P3000 reagent. After cells were seeded for 18 h, the two mixes were combined and kept on ice for 15 min. Then, the cells were incubated with the mixture along with 2 ml of Opti-MEM. After 3 h, FBS was added in a volume corresponding to 10% of the total volume. The cells were incubated with 5 µg/ml of puromycin for 24 h and then washed with PBS, and only the transfected cells were selected. New medium was added to the cells for recovery, and after 24 h, a dilution was performed to obtain a maximum of 600 cells per 12 ml (Figure 9). Diluted cells (100 µl) were then added in each well of three 96-well plate to obtain clonal populations of BV-2 cells. The potential Dpp4 potential mutant / knock-out (KO) cells were validated by Sanger sequencing (Table 1).

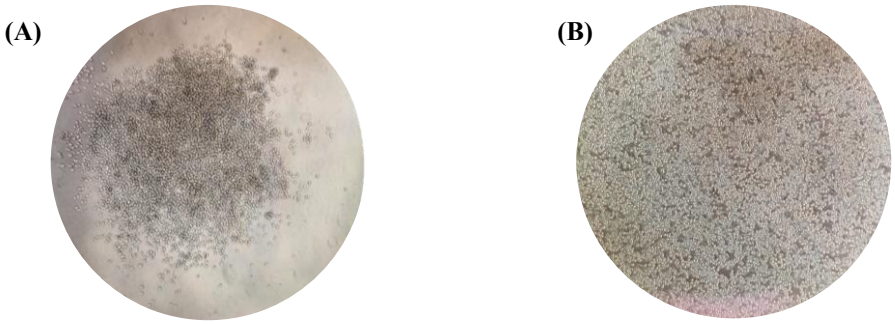

Figure 9 - Deletion of DPP4. (A) Original colony after the 600 cells/12 ml dilution**.** (B) Growing colony.

2.11. DNA extraction

To prepare the DNA samples, proteinase K (0.1 mg/ml) was added to the DNA buffer (100 mM NaCl, 10 mM Tris-HCl, 25 mM EDTA, 5 mM SDS 10%, pH8; 1 µl proteinase K per 100 µl DNA buffer). The cells were pelleted, and the supernatant was discarded before adding the DNA Buffer mix to the cell pellets (300 µl/well). The samples were incubated for 4 h at 56ºC. Following incubation, 300 µl of isopropanol was added and mixed by inverting the tube. After a 15 min centrifugation at 10 000x g, the supernatant was

discarded, and 500 µl of 70% ethanol RNase-free (prepared with RNase-free water) was added to the sample, which was then centrifuged for 10 min (14 000x g). The supernatant was removed, and the pellet was centrifuged again for 5 min. The tubes were then air-dried for 20 min at RT. Finally, 100 µl of DEPC-treated water was added to each sample, and the DNA concentration was measured using a Nanodrop One (ThermoFisher, Scientific, USA).

2.12. RNA extraction

For the ribonucleic acid (RNA) extraction, RNeasy Mini Kit (QIAGEN, Germany) was used according to manufacturer protocol [75]. The cells' medium was collected and centrifuged, and the supernatant was removed while the pellet was mixed with 350 µl Buffer RLT, before being frozen at -20ºC. To disrupt the cells, a syringe (1 ml) and a needle (23G) were used to mix the pellet up and down. The sample was then mixed with 1 volume of 70% ethanol RNase-free, transferred to a RNeasy Mini spin column, and centrifuged for 15 s (8000x g or more), discarding the flow-through after every centrifugation. The spin column was washed twice with 700 µl of Buffer RW1 with a 15 s centrifugation in between, followed by two washes with 500 µl Buffer RPE and a 15 s centrifugation after each wash. After a 2 min centrifugation, the spin column was transferred to a new Eppendorf tube, and 30 µl of RNase-free water (DEPC-treated water) was added. The sample was centrifuged for 1 min, and the amount of RNA in each sample was then quantified with the Nanodrop One (ThermoFisher, Scientific, USA).

2.13. cDNA synthesis

The NZY First-Strand cDNA synthesis kit (NZYTech, Portugal) was employed for cDNA synthesis, according to manufacturer protocol [76]. The procedure was conducted on ice, and the following components were added to a sterile microcentrifuge tube for each sample: 10 µl of NZYRT 2x Master Mix, 2 µl of NZYRT Enzyme Mix, an appropriate volume of RNA to yield up to 5 µg of genetic material in the sample, and RNase-free water to bring the total volume to 20 µl. Subsequently, cDNA samples were appropriately diluted to achieve a final concentration of 25 ng/µl.

2.14. Quantitative reverse transcription PCR (RT-qPCR)

All the required components for this experiment were kept on ice, and the number of tubes needed for the primer mix equalled the number of genes being studied. For the cDNA mix, the number of tubes matched the number of samples plus a negative control (water). Each primer mix consisted of 5 µl of primer F/R (Table 2) and 7.5 µl of DEPC-treated water, while the cDNA mix contained 5 µl of cDNA and 7.5 µl of DEPC-treated water. After adding 5 µl of the primer mix to the PCR plate (ThermoFisher Scientific, USA), the cDNA tubes were supplemented with 25 µl iTaq Universal SYBR Green Supermix (Bio-Rad Laboratories, USA). The contents were mixed, and 15 µl of the mixture were transferred to the plate. The plate was sealed with a MicroAmp Optical Adhesive Film (ThermoFisher Scientific, USA) and centrifuged to eliminate any bubbles. Subsequently, the plate was inserted into the RT-qPCR machine (QuantStudio 3, Applied Biosystems, ThermoFisher Scientific, USA), and information regarding the genes (primers), samples, duplicates, and housekeeping controls was added. The protocol, spanning approximately 2 h, entailed 40 cycles, and consisted of three phases: a hold stage (95ºC for 10 min), a PCR stage (95ºC for 15 s, 60ºC for 45 s, 72ºC for 30 s), and a melt curve stage (95ºC for 15 s, 60ºC for 1 min, 95ºC for 15 s).

The relative quantification of target gene expression was assessed using the comparative threshold (Ct) method, also known as the ΔΔCt method. Ct values were determined for each sample, and subsequently, the ΔCt value was calculated as:

$$\Delta Ct = Ct_{\text{target gene}} - Ct_{\text{housekeeping gene}}.$$

Following that, the ΔΔCt value was determined by the formula:

$$\Delta\Delta Ct = (Ct_{\text{target gene}} - Ct_{\text{housekeeping gene}})_{\text{treated group}} - (Ct_{\text{target gene}} - Ct_{\text{housekeeping gene}})_{\text{control group}}.$$

The relative quantification provides information on the change in the expression of the target gene in treated samples compared to its expression in control samples.

2.15. Statistical analysis

Results are presented as mean ± Standard Error of the Mean (SEM.) Statistical analysis was performed using GraphPad Prism 8.0.2 for Windows. The data were first tested for normality and lognormality distribution. For normally distributed data, an Ordinary one-way ANOVA with Tukey's multiple comparisons test was conducted. For lognormal data, a Kruskal-Wallis' test was employed, followed by uncorrected Dunn's multiple comparison test. Statistical significance was considered at $p<0.05$.

CHAPTER 3

Results

3. Results

In the present work, we aimed to elucidate if sitagliptin can exert direct anti-inflammatory effects on microglial cells. Furthermore, we also intended to clarify if these effects were dependent of the inhibition of DPP4 by sitagliptin, or if other pleiotropic effects could be involved. For this purpose, immortalized microglial cell cultures (BV-2 cell cultures) were exposed to a pro-inflammatory stimulus, LPS, and the effect of sitagliptin in BV-2 cells, expressing or not DPP4, was evaluated.

3.1. Effect of sitagliptin and LPS on BV-2 cells morphology

BV-2 cells were exposed to 200 µM sitagliptin and 0.1 µg/ml LPS. We first assessed whether exposure for 24 h to LPS and/or sitagliptin could affect the viability of BV-2 cells. Phalloidin stained images (Figure 10A) and brightfield images (Figure 10B) show no significant difference between the untreated cells (control condition; CT), and cells treated with 200 µM sitagliptin, 0.1 µg/ml LPS, and 200 µM sitagliptin plus 0.1 µg/ml LPS (Sita +LPS). We conclude that the concentrations of sitagliptin and LPS chosen, do not affect the viability of BV-2 microglial cells.

However, cells exposed to 0.1 µg/ml LPS, a concentration known to trigger BV-2 cells reactivity, are more round shape, which is an indicative of reactive microglial cells.

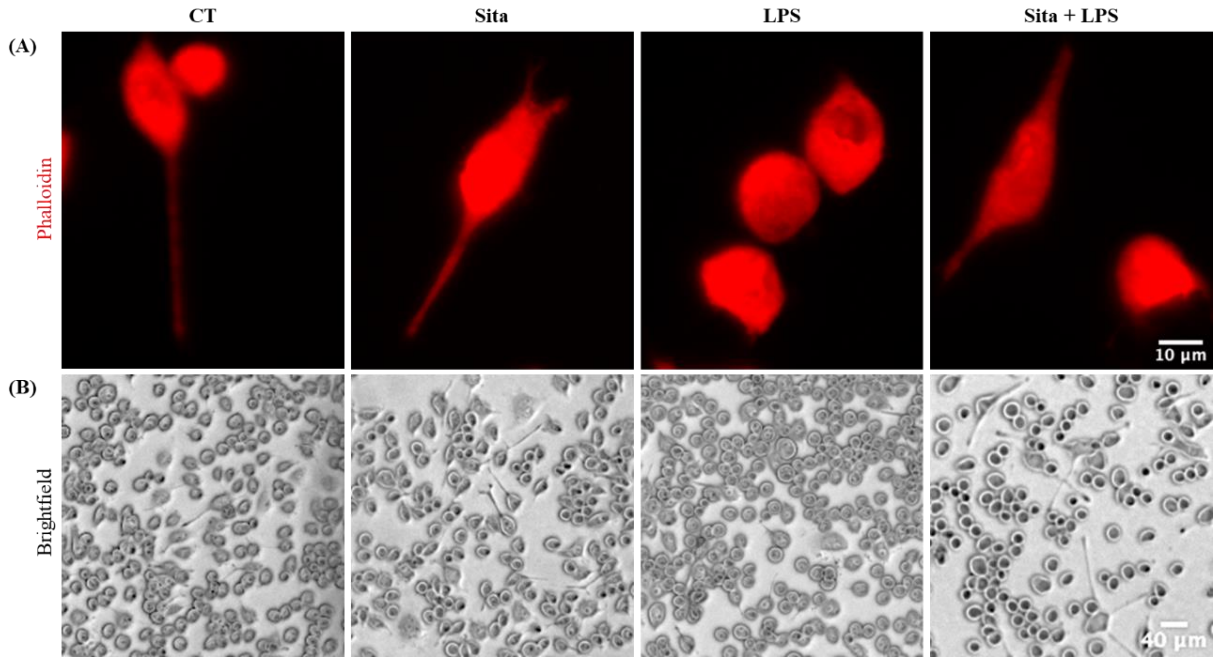

Figure 10 – Effect of sitagliptin and LPS on BV-2 cells morphology. Cells were cultured for 18 h and then exposed to LPS (0.1 µg/ml) for 24 h in the presence or absence of 200 µM sitagliptin. (A) Staining with phalloidin (red) (40X magnification). (B) Brightfield (5X magnification). Scale bar: (A) 10 µm; (B) 40 µm. CT: control; Sita: sitagliptin.

3.2. Sitagliptin does not affect the proliferation rate of BV-2 cells

We also investigated the impact of sitagliptin on the proliferation of microglial cells and its potential safeguarding effect on microglial cells when exposed to LPS, using the EdU assay. This evaluation took place 2 h following the EdU incubation, aiming to determine the percentage of cells incorporating EdU into recently synthesized DNA. (Figure 11A).

As observed, incubating cells with sitagliptin did not affect microglia proliferation, comparing to control. Upon exposure to LPS, the proliferation of BV-2 cells decreased, and this reduction remained unaffected by sitagliptin, indicating that sitagliptin is unable of preventing this decrease (Figure 11B).

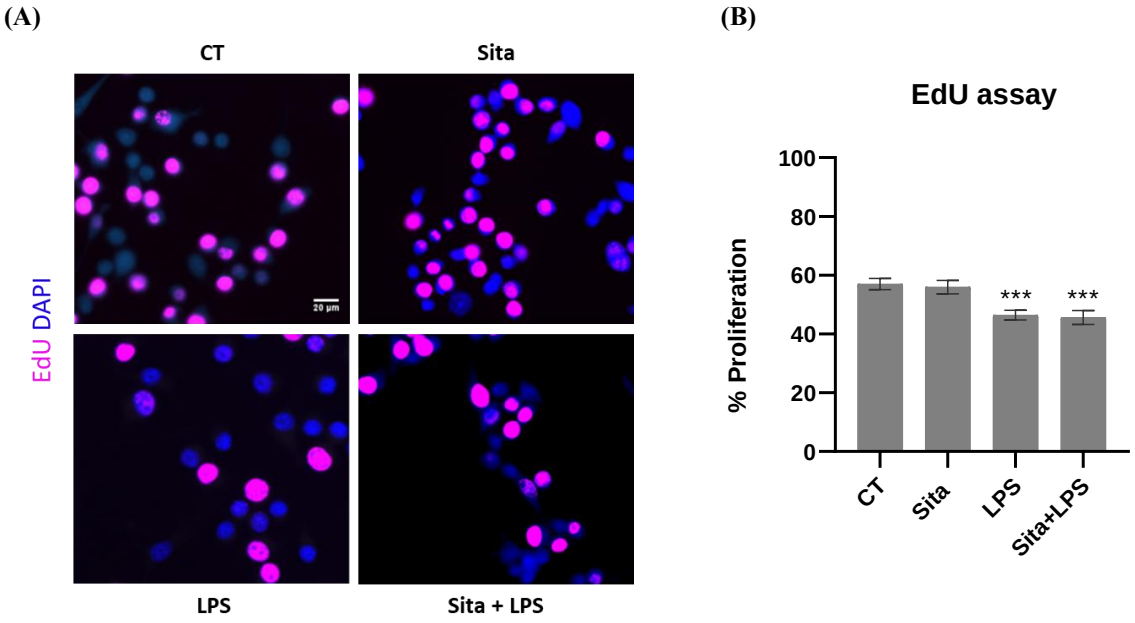

Figure 11 - Sitagliptin does not affect the proliferation of BV-2 cells. Proliferation was evaluated in BV-2 microglial cell cultures using the EdU assay. Cells were exposed to LPS (0.1 µg/ml) for 24 h in the presence or absence of 200 µM sitagliptin. (A) Staining of EdU-positive cells (pink), and cell nuclei with DAPI (blue). Scale bar: 20 µm. (B) The percentage of BV-2 microglial cells proliferating was assessed by counting EdU-positive cells in 5 random fields per experiments (20X magnification). Data are presented as mean ± SEM of 5 independent experiments. CT: control; Sita: sitagliptin. *** $p<0.001$, compared to CT, one-way ANOVA test, followed by Tukey's multiple comparison test.

3.3. Sitagliptin does not induce changes in apoptosis in BV-2 cells

Cleaved caspase-3 is a programmed cell death marker that was used to assess the percentage of apoptotic BV-2 cells after exposure to sitagliptin and/or LPS (Figure 12A). Sitagliptin, LPS and sitagliptin plus LPS did not increase the number of caspase-3-positive cells (Figure 12B). In fact, the number of apoptotic cells in culture was residual. Puromycin was used as a positive control.

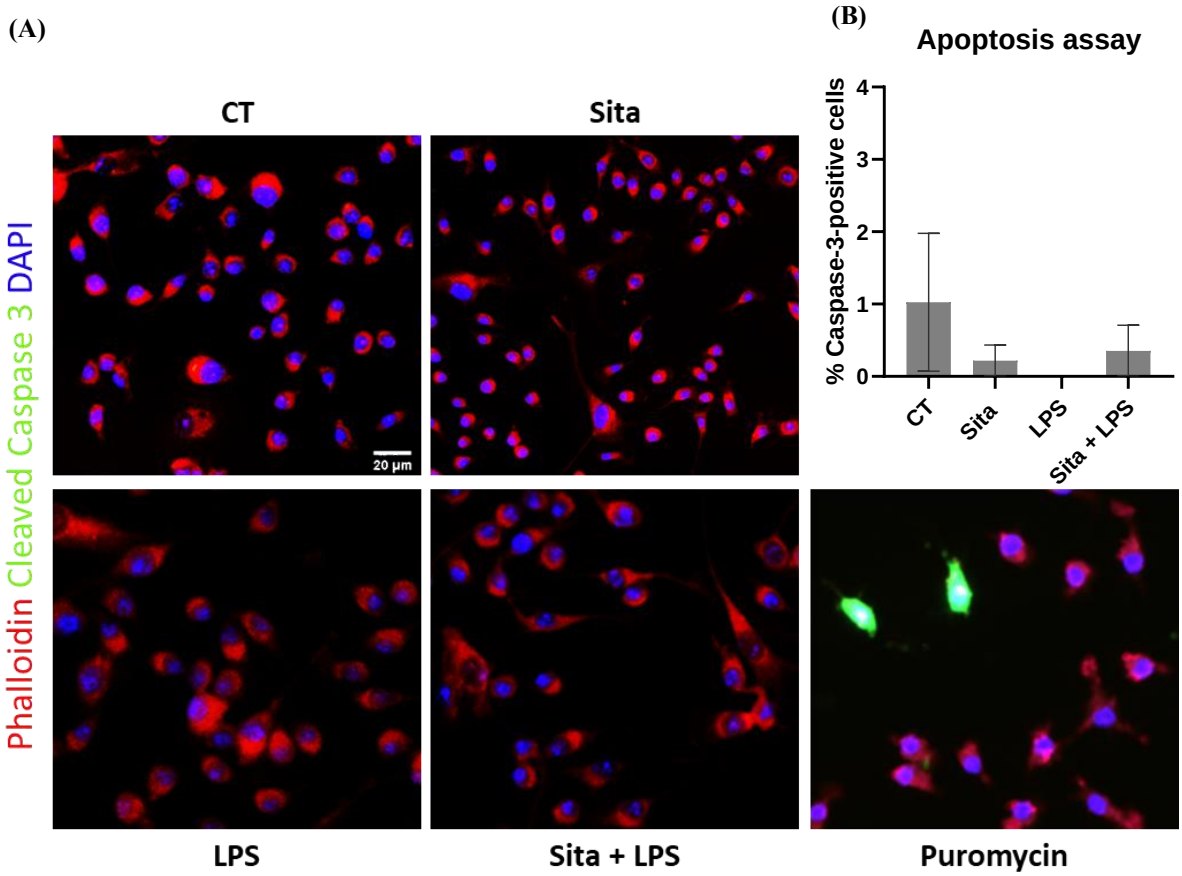

Figure 12 - Sitagliptin does not increase apoptosis in BV-2 cells. Apoptosis was evaluated in BV-2 microglial cell cultures by cleaved caspase 3 immunostaining. Cells were exposed to LPS (0.1 µg/ml) for 24 h in the presence or absence of 200 µM sitagliptin. (A) Immunocytochemistry was performed for cleaved caspase-3 (green). DAPI (blue) was employed for counterstaining the nuclei and phalloidin (red) counterstained the cytoskeleton. Scale bar: 20 µm. (B) The percentage of caspase-3-positive cells was quantified, in 5 random fields per experiment (20X magnification). Data are presented as mean ± SEM of 3 independent experiments. One-way ANOVA test, followed by Tukey's multiple comparison test. CT: control; Sita: sitagliptin.

3.4. Sitagliptin inhibits the upregulation of iNOS, IL-1β and TNF protein levels in BV-2 microglia triggered by exposure to LPS

Microglia can react to pro-inflammatory stimuli by upregulating the expression of pro-inflammatory mediators like iNOS, IL-1β, and TNF. iNOS produces large amounts of nitric oxide, and IL-1β and TNF can be released, thereby enhancing the inflammatory response.

The protein levels of iNOS (Figure 13A), IL-1β (Figure 13B), and TNF (Figure 13C) were quantified by Western Blot in BV-2 microglial cell cultures exposed to LPS, in the absences or presence of sitagliptin. As expected, LPS exposure triggered an increase of iNOS, IL-1β and TNF protein levels, compared to control. The results were normalized to LPS experimental condition (100%), because in some experiments the bands of these proteins in the control condition were barely or even not detected. The presence of sitagliptin significantly inhibited the increase of iNOS, IL-1β and TNF protein levels, triggered by LPS, to 39.35 ± 6.24%, 47.19 ± 8.11%, and 34.02 ± 7.16%, respectively, comparing to LPS.

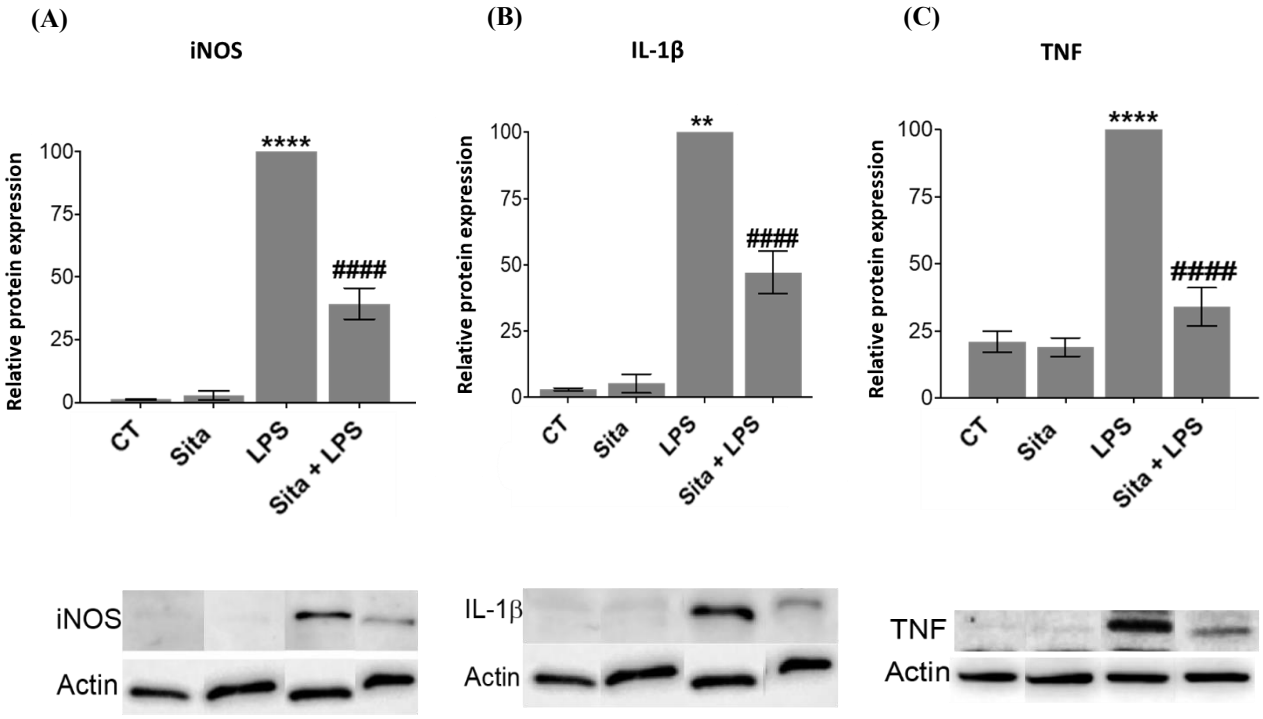

Figure 13 - Sitagliptin inhibits the upregulation of iNOS, IL-1β and TNF protein levels in BV-2 cells triggered by LPS. Protein levels of iNOS (A), IL-1β (B) and TNF (C) were normalized to LPS condition (100%), and to β-actin. Results are presented as mean ± SEM of 3-5 independent experiments. (A, B) ** $p<0.01$ and **** $p<0.0001$, compared to CT; #### $p<0.0001$, compared to LPS; one-way ANOVA, followed by Tukey's multiple comparison test. (C): **** $p<0.0001$, compared to CT; #### $p<0.0001$, compared to LPS; Kruskal-Wallis' test, followed by uncorrected Dunn's test. CT: control; Sita: sitagliptin.

3.5. Sitagliptin inhibits the increase in the phagocytic activity of BV-2 microglia triggered by LPS

Phagocytosis represents a primary function carried out by microglial cells, as it is critically essential for the elimination of apoptotic cells, extracellular protein aggregates, and infectious bacteria. The phagocytosis efficiency of BV-2 cells, pre-treated or not with sitagliptin, and exposed to LPS, was quantified, using fluorescent latex beads (Figure 14A). Microglial cells in culture have basal reactivity and so they incorporate beads, as we can see in the Figure (Figure 14A). The phagocytic efficiency of untreated cells (CT) was very low (20.0 ± 3.3%). The phagocytic efficiency of cells treated with sitagliptin (28.7 ± 7.5%) was similar to the control. In BV-2 cells exposed to LPS there was a significant increase in the number of phagocytized beads (375.0 ± 20.3%; $p<0.0001$), when compared with the control (Figure 14B). However, cells treated with sitagliptin and exposed to LPS presented a significant reduction of the phagocytic efficiency, of approximately 35% (237.8 ± 17.8%; $p<0.0001$), when compared to cells exposed to LPS, indicating that sitagliptin has the capability of reducing the phagocytic efficiency of reactive microglial cells.

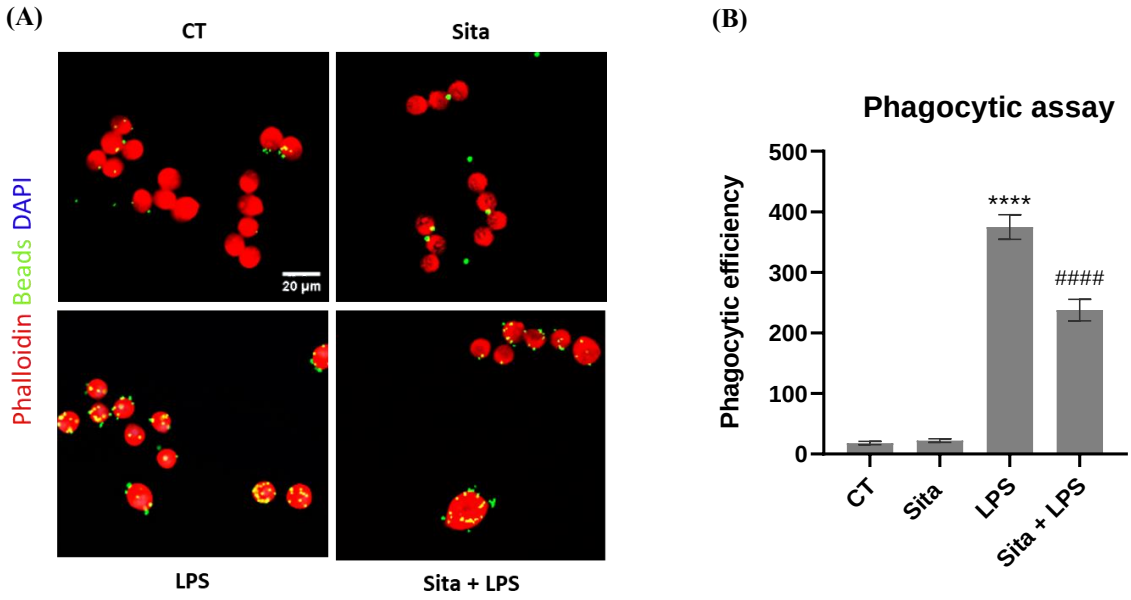

Figure 14 - Sitagliptin inhibits the LPS-induced increase in the phagocytic efficiency of BV-2 microglial cells. (A) Phagocytosis was evaluated in BV-2 microglial cells using fluorescent latex beads (yellow-green). Cells were cultured for 18 h and then exposed to LPS (0.1 µg/ml) for 24 h in the absence or presence of 200 µM sitagliptin. Actin filaments of the cells were stained with phalloidin (red). Scale bar: 20 µm. (B) Phagocytic efficiency was quantified in 5 random fields (20X magnification) of each coverslip, for each independent culture (n=4). Data are presented as mean ± SEM. **** $p<0.0001$, compared to CT; #### $p<0.0001$, compared to LPS; one-way ANOVA test, followed by Tukey's multiple comparison test. CT: control; Sita: sitagliptin.

3.6. BV-2 microglial cells express Dpp4

A major aim of this study was to investigate whether the anti-inflammatory effects of sitagliptin in BV-2 cells were exclusively due to the inhibition of DPP4, or if some pleiotropic effects could be involved. Therefore, it was necessary to make sure that BV-2 microglial cells express DPP4. The presence of Dpp4 mRNA in BV-2 microglial cells was confirmed through RT-PCR analysis (Figure 15). It is possible to observe that Dpp4 mRNA is expressed in untreated cells, as well as in cells treated with sitagliptin and exposed or not to LPS.

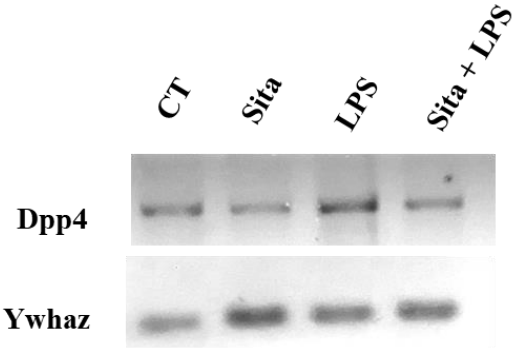

Figure 15 – Dpp4 mRNA is expressed in BV-2 microglial cells. Control BV-2 cells, and cells treated with sitagliptin exposed or not to LPS, express Dpp4. Dpp4 mRNA expression was assessed by RT-PCR. CT: control; Sita: sitagliptin.

3.7. Generation of clones 2 and 31 by CRISPR/Cas9 cloning

Given that Dpp4 mRNA is expressed in BV-2 cells and that sitagliptin is recognized as a DPP4 inhibitor, it becomes imperative to examine whether the sitagliptin's effects on BV-2 inflammatory response triggered by LPS exposure is only mediated by DPP4, or if some pleiotropic effects could be implicated. To achieve this, a CRISPR/Cas9 cloning, Dpp4 deletion and cells transfection, were performed, with the purpose of obtaining Dpp4 knock-out (KO) cells. Several clonal populations of BV-2 cells transfected with pX459 plasmid containing a sgRNA against the exon 3 of Dpp4 were screened by Sanger sequencing. The Sanger sequencing results revealed distinct alterations in the base pair (bp) sequence called indel comparing the WT BV-2 cells and the transfected cells, indicative of a successful gene editing outcome. The success rate of gene editing was superior to 50% generation of indels which is very acceptable for a cell line that is difficult to transfect (10% transfection efficiency with GFP plasmid).

Clone 2 (Figure 16A) and clone 31 (Figure 16B) were selected to perform the experiments. These clones present the addition of a base pair (in pink, Figure 16) at exon 3, in the 5' of the PAM sequence (CCG, in blue, Figure 16) resulting in a change in the reading frame of the target gene and causing a frameshift mutation. Consequently, the encoded protein is likely to be altered, truncated, or not translated, potentially leading to functional changes or loss of function. The difference between these two clones is the base pair added to the sequence, which for clone 2 was a guanine and for clone 31 was an adenine.

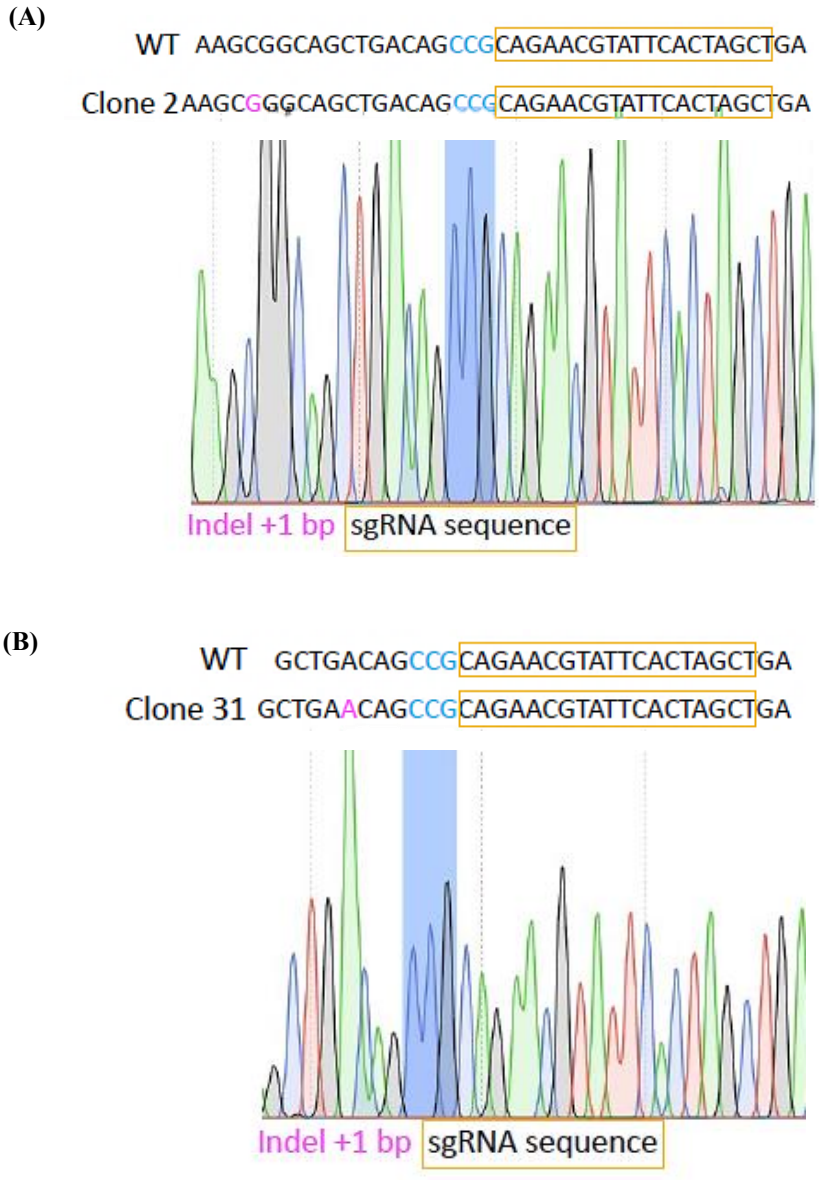

Figure 16 - Sanger sequencing of Dpp4 knock-out clones. CRISPR/Cas9 allowed the generation of two clonal populations of BV-2 cells presenting an indel in the exon 3 of the Dpp4 gene by adding a new base pair: (A) Guanine, in clone 2; and (B) Adenine, in clone 31. In pink: indel; In blue: PAM sequence; Squared in yellow: sgRNA complementary sequence in the exon 3 of Dpp4 gene.

3.8. Dpp4 deletion does not affect the morphology of the BV-2 microglial cells

After making sure that the indel was present in both clones (2 and 31), it was necessary to know whether these clones expressed or not the Dpp4 gene. The Dpp4 mRNA expression was tested by RT-qPCR (Figure 17A). Both clones present almost no Dpp4 mRNA expression, comparing to WT BV-2 microglial. Therefore, clones 2 and 31 were consider as Dpp4 KO.

To test if the deletion of Dpp4 interfere with the cells' morphology, brightfield images were taken of each clone and compared to WT cells (Figure 17B). Clone 2 and clone 31 present similar morphology than WT parentals cells, demonstrating that Dpp4 deletion does not affect the morphology of the cells.

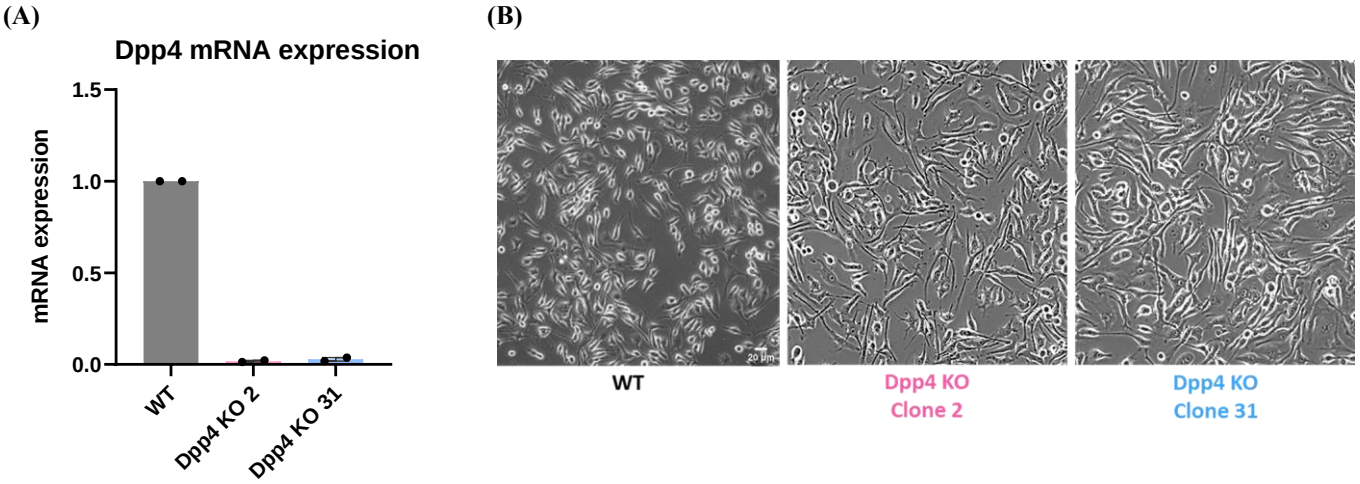

Figure 17 - Characterization of the selected Dpp4 clones. (A) Dpp4 mRNA expression in clones 2 and 31 was assessed by RT-qPCR. Data are presented as mean ± SEM of 2 independent experiments. (B) Morphology of clones 2 and 31 compared to WT BV-2, assessed in brightfield images. Scale bar: 20 µm. Magnification: 10X. WT: wild type; KO: knock-out.

3.9. Dpp4 deletion abolishes the inhibitory effect of sitagliptin on LPS-induced increased in phagocytic activity

Given that sitagliptin significantly inhibited the LPS-induced increase of phagocytic efficiency in WT BV-2 microglia, it is important to examine whether the deletion of Dpp4 in BV-2 microglia impacts on the effect of sitagliptin on phagocytic efficiency.

Non-treated Dpp4 KO cells presented an increase, although not significant, in the number of internalized fluorescent beads, when compared to untreated WT BV-2 cells phagocytic activity (Dpp4 KO 2: 74.98 ± 11.6%; Dpp4 KO 31: 86.83 ± 17.3%; non-significant) (Figure 18A, B, C). When Dpp4 KO BV-2 cells were exposed to LPS, as expected, there was a significant increase in the phagocytic efficiency (Dpp4 KO 2: 325.4 ± 34.3%; Dpp4 KO 31: 329.4 ± 29.3%; $p<0.05$), when compared to untreated KO cells (Figure 18A, B, C).

However, in Dpp4 KO cells treated with sitagliptin and exposed to LPS, the phagocytic efficiency (Dpp4 KO 2: 329.6 ± 55.9%; Dpp4 KO 31: 335.4 ± 51.6%) was similar to that found in Dpp4 KO cells exposed to LPS alone, meaning that, in Dpp4 KO cells, sitagliptin was not able to inhibit the LPS-induced increase in phagocytic efficiency, contrary to what was found in WT BV-2 microglial cells.

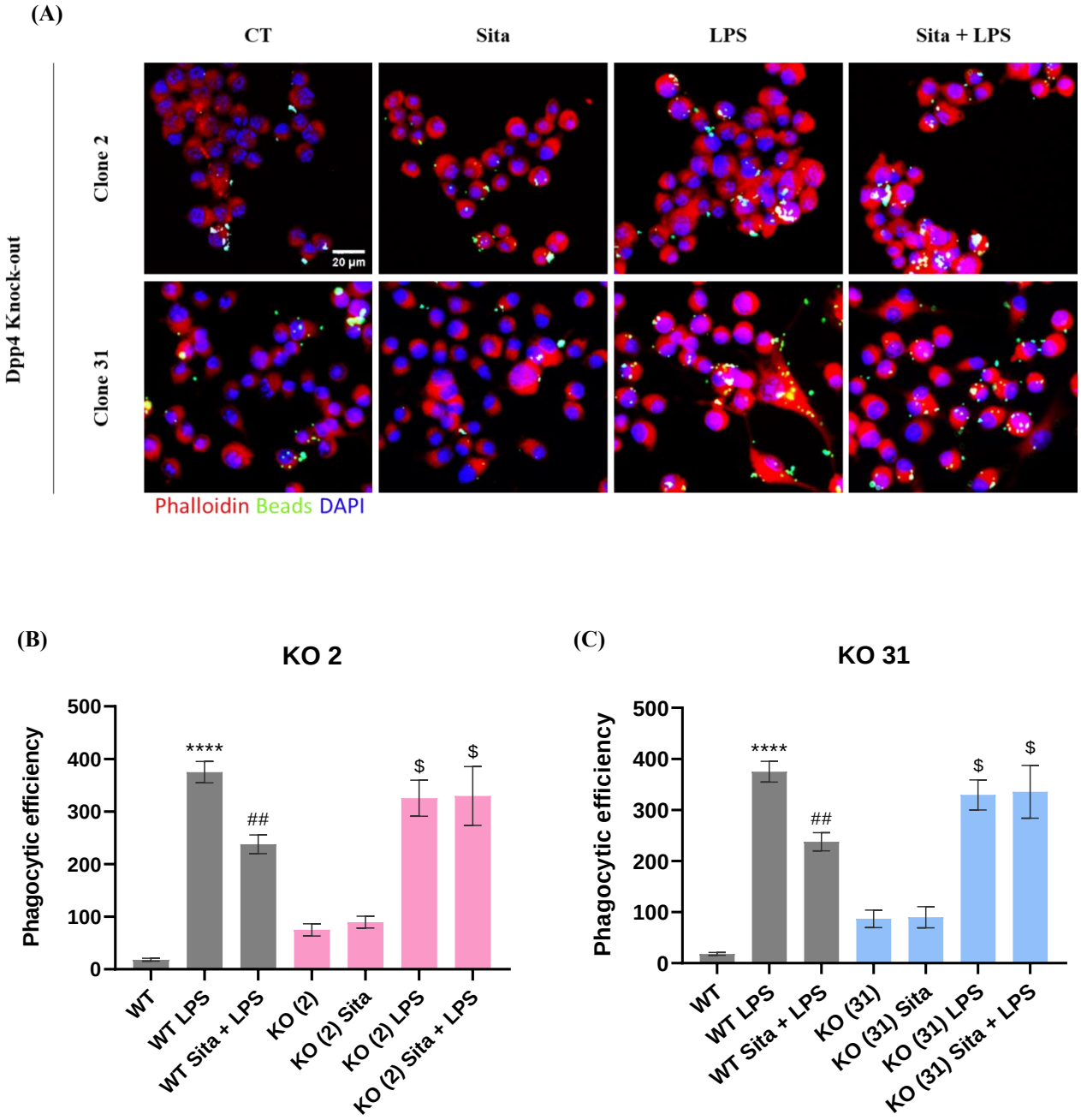

Figure 18 - Dpp4 deletion abolishes the inhibitory effect of sitagliptin on LPS-induced increase in phagocytic efficiency. Phagocytosis was evaluated in Dpp4 KO BV-2 cell cultures using fluorescent latex beads (yellow-green). Cells were exposed to LPS (0.1 µg/ml) for 24 h in the absence or presence of 200 µM sitagliptin. (A) Phalloidin and DAPI staining were used to respectively counterstain the actin filaments (red) and nuclei (blue) of BV-2 cells engulfing the fluorescent latex beads (yellow-green). Scale bar: 20 µm. (B, C) Phagocytic efficiency was quantified in 5 random fields (20X magnification) of each coverslip. Data are presented as mean ± SEM of 5 independent experiments. **** $p<0.0001$, compared to WT; ## $p<0.01$, compared to WT LPS; one-way ANOVA test, followed by Tukey's multiple comparison test. $ $p<0.05$, compared to KO, Kruskal-Wallis's test, followed by uncorrected Dunn's multiple comparison test. WT: wild type; KO: knock-out; Sita: sitagliptin.

CHAPTER 4

Discussion

4. Discussion

Diabetic retinopathy is a chronic neurovascular disorder associated with diabetes, standing as the leading cause of vision impairment and blindness among working-age adults affected by diabetes [1, 2]. This condition arises primarily due to heightened levels of blood glucose and persistent inflammation in the retina, with retinal microglia playing a significant role in its progression [3–8]. In acute injury, microglia become reactive and undertake dual roles of both anti-inflammatory and pro-inflammatory actions. However, under chronic inflammation, the injury becomes persistent, resulting in the ongoing activation of microglia [2, 9–11]. Consequently, under these conditions, there is a gradual decline in anti-inflammatory responses, prompting microglia to shift their role towards promoting inflammation. This alteration leads to the secretion of pro-inflammatory cytokines (such as TNF and IL-1β) and, chemokines, and to the upregulation of iNOS, among others, which together exacerbate diabetic retinopathy. In individuals with diabetes, the levels of pro-inflammatory cytokines and chemokines are elevated in the retina, contributing to retinal cell death and the breakdown of the blood-retinal barrier [16, 17, 32]. Due to these factors and the lack of effective therapies, there is an urgent need to discover solutions, also targeted for the early stages of the disease, that could effectively treat, reverse, or even prevent this condition [12–17].

Sitagliptin is a DPP4 inhibitor that inhibits the cleavage and degradation of incretin hormones. This action leads to elevated levels of these hormones, resulting in increased insulin secretion and reduced glucose production. Our group has reported that sitagliptin has protective and anti-inflammatory effects in the retina, even in a type 1 diabetes animal model, in which sitagliptin effectively prevents the breakdown of the blood-retina barrier. Its mode of action includes the inhibition of the increase of pro-inflammatory cytokine levels, and consequently a reduction of inflammation, as well as the reduction of nitrosative stress and apoptosis. Furthermore, it diminishes the increase of iNOS immunoreactivity in CD11b-positive cells in retinal primary mixed cultures and organotypic cultures, and prevents changes in microglia morphology triggered by exposure to LPS [26–28].

This way, in this study we aimed to test whether sitagliptin has direct anti-inflammatory effects on microglia, and also investigate if the anti-inflammatory effects on microglia are due to the inhibition of DPP4 present in these cells, by using WT BV-2 microglia and Dpp4 KO BV-2 microglia, or if other pleiotropic effects could be involved.

In our research, we assessed the morphology, proliferation, apoptosis, inflammation, and phagocytosis of WT BV-2 microglial cells. These cells were subjected to various conditions: untreated or exposed to LPS, both with and without the presence of sitagliptin. BV-2 cells were employed due to their origin as immortalized neonatal microglia from C57/BL6 mice, making them a commonly used model in scientific investigations. The experimental procedure involved the initial incubation of these cells with sitagliptin to evaluate the drug's capacity to prevent inflammation. Subsequently, the cells were exposed to LPS to induce a pro-inflammatory response. Given the critical role of inflammation in diabetic retinopathy, this approach enabled the assessment of sitagliptin's anti-inflammatory effects specifically on retinal microglia.

The outcomes of our study revealed that sitagliptin did not influence the morphology of BV-2 cells, nor did it impact their proliferation and apoptosis, regardless of LPS exposure. However, we observed that sitagliptin effectively suppressed the elevation of iNOS, IL-1β, and TNF protein levels, as well as the increase of LPS-induced phagocytic activity. These findings align with our previous work showing that sitagliptin prevents nitrosative stress and apoptosis, and the increase of pro-inflammatory cytokines, in the retina of diabetic animals [26, 46].

Furthermore, we demonstrated the presence of Dpp4 mRNA in WT BV-2 microglial cells, untreated or exposed to LPS, in the presence or absence of sitagliptin. This result further support our hypothesis that the anti-inflammatory effect of sitagliptin in the retina is mediated by DPP4 expressed by microglial cells.

To determine whether the effects of sitagliptin on microglia were exclusively dependent on the inhibition of DPP4, or if they could be due to pleiotropic effects, the engineering of Dpp4 KO microglial cells was essential. To accomplish this, parentals (WT) BV-2 were transfected with a plasmid containing a selection marker providing resistance to puromycin (2A-Puro). This plasmid also included the Cas9 gene from S. pyogenes, along with a sgRNA targeting the exon 3 of the Dpp4 gene. We initially ensured the presence of indels in multiple clones through Sanger sequencing. Subsequently, two distinct clones (clone 2 and clone 31) were chosen. Both have an indel at exon 3, allowing the alteration in the reading frame of the target gene, resulting in a frameshift mutation. The cell morphology and Dpp4 mRNA expression of both clones were assessed.

Our findings not only revealed an almost negligible Dpp4 mRNA expression in these two clones, indicating the successful generation of Dpp4 KO cells, but also highlighted

that their morphology remained practically unchanged being similar to WT parentals cells, which means that Dpp4 deletion does not affect the morphology of Dpp4 KO cells.

Subsequent to this step, we faced uncertainty regarding the outcomes of the remaining experiments involving these KO cells, given the scarce available literature on experiments involving Dpp4 KO cells. Though, we hypothesized that without the presence of DPP4 in microglial cells, and once sitagliptin is a DPP4 inhibitor, sitagliptin no longer could exert effects on microglia cells and, consequently, on inflammatory responses by microglia.

Therefore, we investigated the phagocytic activity of non-treated Dpp4 KO clones, through which we observed that there was an increase of their phagocytic activity, comparing with WT cells, but non-statistically significant. Moreover, the deletion of Dpp4 did not significantly affect the phagocytic efficiency in cells exposed to LPS, when compared to WT cells. However, and importantly, sitagliptin lost the inhibitory effect on the increase in the phagocytic efficiency induced by LPS, clearly indicating that, at least regarding the phagocytic activity, the effects of sitagliptin were mediated exclusively by the inhibition of DPP4, present in BV-2 cells.

Nonetheless, to substantiate the influence of Dpp4 deletion on the protective effects of sitagliptin, additional experiments, and a scientific acceptable number of independent experiments for each assay, are still necessary to assess various parameters in the Dpp4 KO cells.

Based on the findings from this investigation, it can be asserted that sitagliptin is a specific inhibitor of DPP4. However, this specificity does not preclude the possibility that even when inhibited, some DPP4 proteins could still interact with other proteins, such as the adenosine deaminase, to induce an anti-inflammatory effect, but this still needs to be further explored.

In summary, it can be asserted that sitagliptin exerts direct effects on microglia and has anti-inflammatory effects on these cells. Data with the Dpp4 KO clones presented here, and some rather preliminary not shown here, suggest that the sitagliptin anti-inflammatory effects can be mediated, almost exclusively, by the DPP4 inhibition, but we cannot completely exclude the involvement of some pleiotropic effects.

CHAPTER 5

Conclusions and Future Directions

5. Conclusions and future directions

The results obtained in this study allowed drawing the following main conclusions:

- BV-2 cells express Dpp4;
- Sitagliptin inhibits the LPS-triggered upregulation of iNOS, IL-1β and TNF protein levels, as well as the phagocytic activity, in BV-2 cells, confirming that sitagliptin is able to induce anti-inflammatory effects;
- Sitagliptin exerts direct effects on microglial cells;
- Dpp4 deletion does not significantly affect the morphology of BV-2 cells;
- The inhibitory effect of sitagliptin on LPS-induced increase in phagocytic efficiency in BV-2 cells is lost when Dpp4 is deleted, indicating that the effect of sitagliptin was mediated by the inhibition of DPP4.

The results obtained in this study suggest that the anti-inflammatory effects of sitagliptin in BV-2 microglia are essentially mediated by the selective inhibition of DPP4. However, since other parameters need to be evaluated in the future, it remains to be clarified whether the anti-inflammatory properties of sitagliptin are exclusively dependent on its interaction with DPP4, or if it exerts other pleiotropic effects.

Regarding future perspectives, it is imperative to research deeper into the mechanisms underlying the anti-inflammatory effects of sitagliptin. The investigation should aim to identify the molecules that may interact with sitagliptin and/or DPP4, and consequently the pathways involved, uncovering the underlying mechanisms through which sitagliptin exerts its proven anti-inflammatory effects.

CHAPTER 6

References

6. References

1. T. Oshitari, “Neurovascular impairment and therapeutic strategies in diabetic retinopathy,” *Int. J. Environ. Res. Public Health*, vol. 19, no. 1, 2022, doi: 10.3390/ijerph19010439.
2. F. Gui, Z. You, S. Fu, H. Wu, and Y. Zhang, “Endothelial Dysfunction in Diabetic Retinopathy,” *Front. Endocrinol. (Lausanne).*, vol. 11, p. 591, Sep. 2020, doi: 10.3389/FENDO.2020.00591.
3. “Diabetic Retinopathy | National Eye Institute.” https://www.nei.nih.gov/learn-about-eye-health/eye-conditions-and-diseases/diabetic-retinopathy (accessed Jan. 11, 2023).
4. “Diabetic Retinopathy | Johns Hopkins Medicine.” https://www.hopkinsmedicine.org/health/conditions-and-diseases/diabetes/diabetic-retinopathy (accessed Jan. 11, 2023).
5. “Diabetic Retinopathy Treatment | Stanford Health Care.” https://stanfordhealthcare.org/medical-conditions/eyes-and-vision/diabetic-retinopathy/treatments.html (accessed Jan. 12, 2023).
6. J. M. Grabham, “Vitrectomy surgery.,” *Nurs. Times*, vol. 78, no. 50, pp. 2113–2117, 1982.
7. K. Y. Lin, W. H. Hsih, Y. B. Lin, C. Y. Wen, and T. J. Chang, “Update in the epidemiology, risk factors, screening, and treatment of diabetic retinopathy,” *J. Diabetes Investig.*, vol. 12, no. 8, pp. 1322–1325, 2020, doi: 10.1111/jdi.13480.
8. W. Wang and A. C. Y. Lo, “Diabetic retinopathy: Pathophysiology and treatments,” *Int. J. Mol. Sci.*, vol. 19, no. 6, 2018, doi: 10.3390/ijms19061816.
9. H. Xu, W. T. Wong, P. Sapieha, T. Langmann, K. Rashid, and I. Akhtar-Schaefer, “Microglia in Retinal Degeneration,” *Front. Immunol. | www.frontiersin.org*, vol. 1, 2019, doi: 10.3389/fimmu.2019.01975.
10. W. Ma, L. Zhao, and W. T. Wong, “Microglia in the Outer Retina and their Relevance to Pathogenesis of Age-Related Macular Degeneration (AMD),” *Adv. Exp. Med. Biol.*, vol. 723, p. 37, 2012, doi: 10.1007/978-1-4614-0631-0_6.
11. X. Fu, S. Feng, H. Qin, L. Yan, C. Zheng, and K. Yao, “Microglia: The breakthrough to treat neovascularization and repair blood-retinal barrier in retinopathy,” *Front. Mol. Neurosci.*, vol. 16, Jan. 2023, doi: 10.3389/FNMOL.2023.1100254.
12. Y. Tomita, D. Lee, K. Tsubota, K. Negishi, and T. Kurihara, “Updates on the Current

Treatments for Diabetic Retinopathy and Possibility of Future Oral Therapy," *J. Clin. Med.*, vol. 10, no. 20, Oct. 2021, doi: 10.3390/JCM10204666.

13. R. A. Kowluru and S. Odenbach, "Role of interleukin-1β in the pathogenesis of diabetic retinopathy," *Br. J. Ophthalmol.*, vol. 88, no. 10, p. 1343, Oct. 2004, doi: 10.1136/BJO.2003.038133.
14. J. Adamiec-Mroczek and J. Oficjalska-Młyńczak, "Assessment of selected adhesion molecule and proinflammatory cytokine levels in the vitreous body of patients with type 2 diabetes-role of the inflammatory-immune process in the pathogenesis of proliferative diabetic retinopathy", doi: 10.1007/s00417-008-0868-6.
15. I. D. Aires *et al.*, "Blockade of microglial adenosine A 2A receptor suppresses elevated pressure-induced inflammation, oxidative stress, and cell death in retinal cells," *Glia*, vol. 67, no. 5, pp. 896–914, 2019, doi: 10.1002/glia.23579.
16. E. C. Leal *et al.*, "Inducible Nitric Oxide Synthase Isoform Is a Key Mediator of Leukostasis and Blood-Retinal Barrier Breakdown in Diabetic Retinopathy," *Invest. Ophthalmol. Vis. Sci.*, vol. 48, no. 11, pp. 5257–5265, Nov. 2007, doi: 10.1167/IOVS.07-0112.
17. J. Tang and T. S. Kern, "Inflammation in Diabetic Retinopathy," *Prog. Retin. Eye Res.*, vol. 30, no. 5, p. 343, Sep. 2011, doi: 10.1016/J.PRETEYERES.2011.05.002.
18. J. Huang *et al.*, "Emerging Role of Dipeptidyl Peptidase-4 in Autoimmune Disease," *Front. Immunol.*, vol. 13, p. 830863, Mar. 2022, doi: 10.3389/FIMMU.2022.830863/BIBTEX.
19. N. Enz, G. Vliegen, I. De Meester, and W. Jungraithmayr, "CD26/DPP4 - a potential biomarker and target for cancer therapy," *Pharmacol. Ther.*, vol. 198, pp. 135–159, Jun. 2019, doi: 10.1016/J.PHARMTHERA.2019.02.015.
20. X. Hu, X. Wang, and X. Xue, "Therapeutic Perspectives of CD26 Inhibitors in Imune-Mediated Diseases," *Molecules*, vol. 27, no. 14, Jul. 2022, doi: 10.3390/MOLECULES27144498.
21. R. Nistala and V. Savin, "Diabetes, hypertension, and chronic kidney disease progression: Role of DPP4," *Am. J. Physiol. - Ren. Physiol.*, vol. 312, no. 4, pp. F661–F670, Apr. 2017, doi: 10.1152/AJPRENAL.00316.2016/ASSET/IMAGES/LARGE/ZH20031781630002.JPEG.
22. T. Zhang *et al.*, "The Roles of Dipeptidyl Peptidase 4 (DPP4) and DPP4 Inhibitors in Different Lung Diseases: New Evidence," *Front. Pharmacol.*, vol. 12, Dec. 2021, doi:

10.3389/FPHAR.2021.731453.

23. C. F. Deacon, “Physiology and Pharmacology of DPP-4 in Glucose Homeostasis and the Treatment of Type 2 Diabetes,” *Front. Endocrinol. (Lausanne).*, vol. 10, p. 440649, Feb. 2019, doi: 10.3389/FENDO.2019.00080/BIBTEX.
24. T. Iwanaga and J. Nio-Kobayashi, “Cellular expression of CD26/dipeptidyl peptidase IV,” *Biomed. Res.*, vol. 42, no. 6, pp. 229–237, 2021, doi: 10.2220/BIOMEDRES.42.229.
25. D. Röhrborn, N. Wronkowitz, and J. Eckel, “DPP4 in Diabetes,” *Front. Immunol.*, vol. 6, no. JUL, p. 386, 2015, doi: 10.3389/FIMMU.2015.00386.
26. A. Gonçalves *et al.*, “Protective effects of the dipeptidyl peptidase IV inhibitor sitagliptin in the blood-retinal barrier in a type 2 diabetes animal model,” *Diabetes, Obes. Metab.*, vol. 14, no. 5, pp. 454–463, 2012, doi: 10.1111/j.1463-1326.2011.01548.x.
27. A. Gonçalves *et al.*, “The dipeptidyl peptidase-4 (DPP-4) inhibitor sitagliptin ameliorates retinal endothelial cell dysfunction triggered by inflammation,” *Biomed. Pharmacother.*, vol. 102, no. March, pp. 833–838, 2018, doi: 10.1016/j.biopha.2018.03.144.
28. S. R. F. G. Correia, “Involvement of the NPY system in the inflammatory responses mediated by retinal microglial cells : modulation by sitagliptin,” 2014.
29. A. R. Santiago *et al.*, “Role of microglia adenosine A2A receptors in retinal and brain neurodegenerative diseases,” *Mediators Inflamm.*, vol. 2014, no. 2, 2014, doi: 10.1155/2014/465694.
30. “Diabetes.” https://www.who.int/news-room/fact-sheets/detail/diabetes (accessed Jan. 11, 2023).
31. V. Ingle and P. Ambad, “Diabetic retinopathy classifier with convolution neural network,” *Mater. Today Proc.*, no. xxxx, 2022, doi: 10.1016/j.matpr.2022.09.480.
32. A. M. A. El-Asrar, “Role of Inflammation in the Pathogenesis of Diabetic Retinopathy,” *Middle East Afr. J. Ophthalmol.*, vol. 19, no. 1, p. 70, Jan. 2012, doi: 10.4103/0974-9233.92118.
33. C. Altmann and M. H. H. Schmidt, “The Role of Microglia in Diabetic Retinopathy: Inflammation, Microvasculature Defects and Neurodegeneration,” *Int. J. Mol. Sci.*, vol. 19, no. 1, Jan. 2018, doi: 10.3390/IJMS19010110.
34. S. Paulo, “Daniella do Carmo Buonfiglio Estudo da síntese de melatonina em retinas de ratos Wistar diabéticos,” 2010.

35. D. Purves *et al.*, *Neuroscience Third Edition*. 2019. doi: 10.1016/B978-0-12-801238-3.62132-3.

36. C. Roubeix, J. A. Sahel, X. Guillonneau, C. Delarasse, and F. Sennlaub, "On the inflammatory origins of AMD," *Medecine/Sciences*, vol. 36, no. 10, pp. 886–892, 2020, doi: 10.1051/medsci/2020094.

37. K. Baba, V. Goyal, and G. Tosini, "Circadian Regulation of Retinal Pigment Epithelium Function," *Int. J. Mol. Sci.*, vol. 23, no. 5, p. 2699, Mar. 2022, doi: 10.3390/IJMS23052699.

38. R. Sharma, D. Bose, A. Maminishkis, and K. Bharti, "RETINAL PIGMENT EPITHELIUM REPLACEMENT THERAPY FOR AGE-RELATED MACULAR DEGENERATION – ARE WE THERE YET?," *Annu. Rev. Pharmacol. Toxicol.*, vol. 60, p. 553, Jan. 2020, doi: 10.1146/ANNUREV-PHARMTOX-010919-023245.

39. C. Zhang, H. Wang, J. Nie, and F. Wang, "Protective Factors in Diabetic Retinopathy: Focus on Blood-Retinal Barrier," *Discov. Med.*, vol. 18, no. 98, pp. 105–112, Sep. 2014.

40. G. Rathnasamy, W. S. Foulds, E. A. Ling, and C. Kaur, "Retinal microglia – A key player in healthy and diseased retina," *Prog. Neurobiol.*, vol. 173, no. May 2018, pp. 18–40, 2019, doi: 10.1016/j.pneurobio.2018.05.006.

41. "Retina - Anatomia do Olho - Visão - InfoEscola." https://www.infoescola.com/visao/retina/ (accessed Oct. 10, 2022).

42. A. Naylor, A. Hopkins, N. Hudson, and M. Campbell, "Tight Junctions of the Outer Blood Retina Barrier," *Int. J. Mol. Sci.*, vol. 21, no. 1, Jan. 2020, doi: 10.3390/IJMS21010211.

43. F. O'Leary and M. Campbell, "The blood–retina barrier in health and disease," *FEBS J.*, vol. 290, no. 4, pp. 878–891, 2023, doi: 10.1111/febs.16330.

44. J. Cunha-Vaz, R. Bernardes, and C. Lobo, "Blood-retinal barrier," *Eur. J. Ophthalmol.*, vol. 21, no. SUPPL.6, pp. 3–9, 2011, doi: 10.5301/EJO.2010.6049.

45. M. Chen, C. Luo, J. Zhao, G. Devarajan, and H. Xu, "Immune regulation in the aging retina," *Prog. Retin. Eye Res.*, vol. 69, p. 159, Mar. 2019, doi: 10.1016/J.PRETEYERES.2018.10.003.

46. A. Gonçalves *et al.*, "Dipeptidyl peptidase-IV inhibition prevents blood-retinal barrier breakdown, inflammation and neuronal cell death in the retina of type 1 diabetic rats," *Biochim. Biophys. Acta - Mol. Basis Dis.*, vol. 1842, no. 9, pp. 1454–1463, 2014, doi: 10.1016/j.bbadis.2014.04.013.

47. D. Goldman, “Müller glia cell reprogramming and retina regeneration,” *Nat. Rev. Neurosci.*, vol. 15, no. 7, p. 431, 2014, doi: 10.1038/NRN3723.
48. L. Fernández-Sánchez, P. Lax, L. Campello, I. Pinilla, and N. Cuenca, “Astrocytes and Müller cell alterations during retinal degeneration in a transgenic rat model of retinitis pigmentosa,” *Front. Cell. Neurosci.*, vol. 9, no. DEC, p. 163624, Dec. 2015, doi: 10.3389/FNCEL.2015.00484/BIBTEX.
49. H. Kolb, “Glial Cells of the Retina,” *Webvision Organ. Retin. Vis. Syst.*, Apr. 2007, Accessed: Aug. 03, 2023. [Online]. Available: https://www.ncbi.nlm.nih.gov/books/NBK11516/
50. G. N. Costa, J. Vindeirinho, C. Cavadas, A. F. Ambrósio, and P. F. Santos, “Contribution of TNF receptor 1 to retinal neural cell death induced by elevated glucose,” *Mol. Cell. Neurosci.*, vol. 50, no. 1, pp. 113–123, May 2012, doi: 10.1016/J.MCN.2012.04.003.
51. J. Lechner, O. E. O’Leary, and A. W. Stitt, “The pathology associated with diabetic retinopathy,” *Vision Res.*, vol. 139, pp. 7–14, Oct. 2017, doi: 10.1016/J.VISRES.2017.04.003.
52. R. Simó, A. W. Stitt, and T. W. Gardner, “Neurodegeneration in diabetic retinopathy: does it really matter?,” *Diabetologia*, vol. 61, no. 9, p. 1902, Sep. 2018, doi: 10.1007/S00125-018-4692-1.
53. M. M. Sachdeva, “Retinal Neurodegeneration in Diabetes: an Emerging Concept in Diabetic Retinopathy,” *Curr. Diab. Rep.*, vol. 21, no. 12, p. 3, Dec. 2021, doi: 10.1007/S11892-021-01428-X.
54. A. J. Barber and B. Baccouche, “Neurodegeneration in diabetic retinopathy: Potential for novel therapies,” *Vision Res.*, vol. 139, pp. 82–92, Oct. 2017, doi: 10.1016/J.VISRES.2017.06.014.
55. U. M. Kinuthia, A. Wolf, and T. Langmann, “Microglia and Inflammatory Responses in Diabetic Retinopathy,” *Front. Immunol.*, vol. 11, no. November, pp. 1–10, 2020, doi: 10.3389/fimmu.2020.564077.
56. J. G. Grigsby *et al.*, “The Role of Microglia in Diabetic Retinopathy,” *J. Ophthalmol.*, vol. 2014, 2014, doi: 10.1155/2014/705783.
57. X. Huang, Y. Tong, C. X. Qi, H. D. Dan, Q. Q. Deng, and Y. Shen, “Large-Scale Neuronal Network Dysfunction in Diabetic Retinopathy,” *Neural Plast.*, vol. 2020, 2020, doi: 10.1155/2020/6872508.
58. “021995s000_MedR.pdf.”

59. L. J. Scott, “Sitagliptin: A Review in Type 2 Diabetes,” *Drugs*, vol. 77, no. 2, pp. 209–224, Feb. 2017, doi: 10.1007/S40265-016-0686-9/FIGURES/1.

60. “Sitagliptin (Oral Route) - Mayo Clinic.” https://www.mayoclinic.org/drugs./sitagliptin./drg-20069730?p=1 (accessed May 16, 2023).

61. K. Makrilakis, “The Role of DPP-4 Inhibitors in the Treatment Algorithm of Type 2 Diabetes Mellitus: When to Select, What to Expect,” *Int. J. Environ. Res. Public Heal. 2019, Vol. 16, Page 2720*, vol. 16, no. 15, p. 2720, Jul. 2019, doi: 10.3390/IJERPH16152720.

62. “Sitagliptin | C16H15F6N5O | CID 4369359 - PubChem.” https://pubchem.ncbi.nlm.nih.gov/compound/Sitagliptin (accessed Aug. 03, 2023).

63. N. Enz, G. Vliegen, I. De Meester, and W. Jungraithmayr, “CD26/DPP4-a potential biomarker and target for cancer therapy,” 2019, doi: 10.1016/j.pharmthera.2019.02.015.

64. M. H. Madeira, R. Boia, P. F. Santos, A. F. Ambrósio, and A. R. Santiago, “Contribution of Microglia-Mediated Neuroinflammation to Retinal Degenerative Diseases,” *Mediators Inflamm.*, vol. 2015, 2015, doi: 10.1155/2015/673090.

65. F. I. Baptista, C. A. Aveleira, Á. F. Castilho, and A. F. Ambrósio, “Elevated Glucose and Interleukin-1β Differentially Affect Retinal Microglial Cell Proliferation,” *Mediators Inflamm.*, vol. 2017, 2017, doi: 10.1155/2017/4316316.

66. I. D. Aires *et al.*, “Exosomes derived from microglia exposed to elevated pressure amplify the neuroinflammatory response in retinal cells,” *Glia*, vol. 68, no. 12, pp. 2705–2724, Dec. 2020, doi: 10.1002/GLIA.23880.

67. I. D. Aires *et al.*, “Intravitreal injection of adenosine A2A receptor antagonist reduces neuroinflammation, vascular leakage and cell death in the retina of diabetic mice,” *Sci. Rep.*, vol. 9, no. 1, Dec. 2019, doi: 10.1038/S41598-019-53627-Y.

68. A. Henn, S. Lund, M. Hedtjärn, A. Schrattenholz, E. Pörzgen, and M. Leist, “The Suitability of BV2 Cells as Alternative Model System for Primary Microglia Cultures or for Animal Experiments Examining Brain Inflammation,” vol. 25, no. 1, pp. 89–92, 1973, doi: 10.1007/BF01085399.

69. M. A. Laurenzi, C. Arcuri, R. Rossi, P. Marconi, and V. Bocchini, “Effects of Microenvironment on Morphology and Function of the Microglial Cell Line BV-2,” *Neurochem. Res.*, vol. 26, no. 11, pp. 1209–1216, 2001.

70. R. J. Horvath, N. Nutile-McMenemy, M. S. Alkaitis, and J. A. DeLeo, “Differential

migration, LPS-induced cytokine, chemokine and NO expression in immortalized BV-2 and HAPI cell lines and primary microglial cultures," *J. Neurochem.*, vol. 107, no. 2, p. 557, Oct. 2008, doi: 10.1111/J.1471-4159.2008.05633.X.

71. "BV-2 Microglial Cells | AcceGen." https://www.accegen.com/product/bv-2-abc-tc212s/ (accessed May 30, 2023).
72. I. Las, "ImageQuantLAS500".
73. NZY Tech, "Supreme NZYTaq II 2 × Green Master Mix," p. 2, 2017, [Online]. Available: https://www.nzytech.com/products-services/pcr-master-mixes/mb360/
74. ThermoFisher, "Lipofectamine 3000 Reagent Protocol".
75. R. M. Kit, "RNeasy ® Mini Kit, Part 1," no. November, pp. 3–4, 2021.
76. NZYTech – Genes & Enzymes, "Product Brochure: NZY First-Strand cDNA Synthesis Kit, Catalogue number: MB12501, 50 reactions; MB12502, 250 reactions," vol. 12501, no. 1, [Online]. Available: https://www.nzytech.com/products-services/molecular-biology/rna-cdna/cdna-synthesis/cdna-kits/mb125/